Aerodynamics and Aircraft Control

3

3.1 Introduction

The objective of this chapter is to provide the reader with an introduction to aerodynamics, aircraft stability and control and the dynamic response and behaviour of an aircraft so as to be able to understand the role and tasks of automatic flight control systems. The aim is to establish the essential background to fly-by-wire (FBW) flight control (Chap. 4) and autopilots (Chap. 8).

3.2 Basic Aerodynamics

Most readers will be aware of the basic principles of aircraft flight and how the wings generate lift to support the weight of the aircraft. The aerodynamic aspects of aircraft flight are thus covered briefly, principally to recap and define the terms and aerodynamic parameters which are used.

3.2.1 Lift and Drag

An aerofoil inclined at an angle to a moving air stream will experience a resultant force due to aerodynamic effects. This resultant aerodynamic force is generated by the following:

(a) A reduction in the pressure over the upper surface of the wing as the airflow speeds up to follow the wing curvature, or camber.
(b) An increase in pressure on the undersurface of the wing due to the impact pressure of the component of the air stream at right angles to the undersurface.

About two-thirds of this resultant aerodynamic force is due to the reduction in pressure over the upper surface of the wing and about one-third due to the increase in pressure on the lower surface. Fig. 3.1 illustrates the pressure distribution over a typical aerofoil.

The aerodynamic force exerted on an aerofoil can also be explained as being the reaction force resulting from the rate of change of momentum of the moving air stream by the action of the aerofoil in deflecting the airstream from its original direction (see Fig. 3.2).

The ability of an aerofoil to deflect a stream of air depends on the angle between the aerofoil and the airstream and on the curvature, or camber, of the aerofoil. The aerodynamic force is increased by increasing the camber or by increasing the angle between the aerofoil and the airstream. The thickness of the aerofoil also determines how efficiently the aerofoil produces a force.

This resultant aerodynamic force can be resolved into two components. The component at right angles to the velocity of the air relative to the wing (generally referred to in aerodynamic textbooks as *relative wind*) is called the *lift force*.

The component parallel to the air velocity is known as the *drag force* and, as its name implies, acts on the wing in the opposite sense to the velocity of the wing relative to the air mass (or alternatively in the direction of the relative wind). It should be noted that the drag force component of the aerodynamic force acting on the wing is known as the *wing drag* and constitutes a large part of the total drag acting on the aircraft particularly at high angles of incidence.

3.2.2 Angle of Incidence/Angle of Attack

Referring to Fig. 3.3, the angle between the direction of the air velocity relative to the wing (relative wind) and the wing chord line (a datum line through the wing section) is known both as the *angle of incidence* and as the *angle of attack*. Angle of incidence is the term generally used in the UK and angle of attack in the USA. Angle of incidence is used in this book.

R. P. G. Collinson, *Introduction to Avionics Systems*, https://doi.org/10.1007/978-3-031-29215-6_3

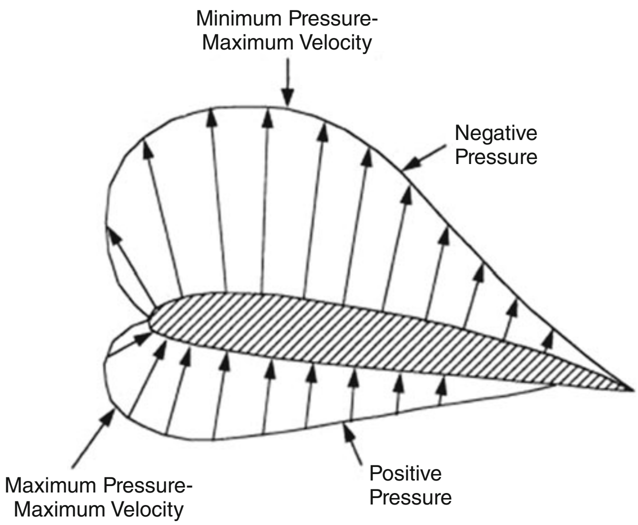

Fig. 3.1 Pressure distribution over an aerofoil

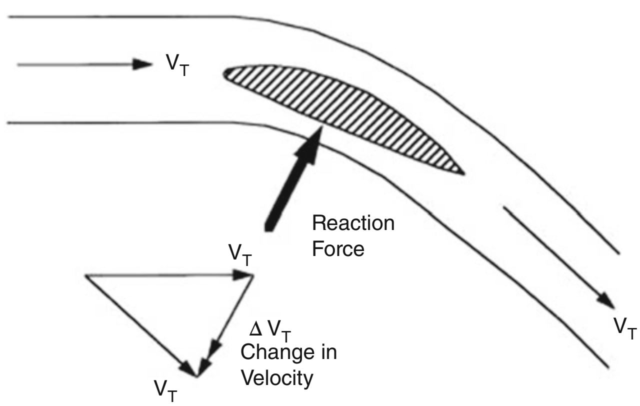

Fig. 3.2 Change in airflow momentum by aerofoil

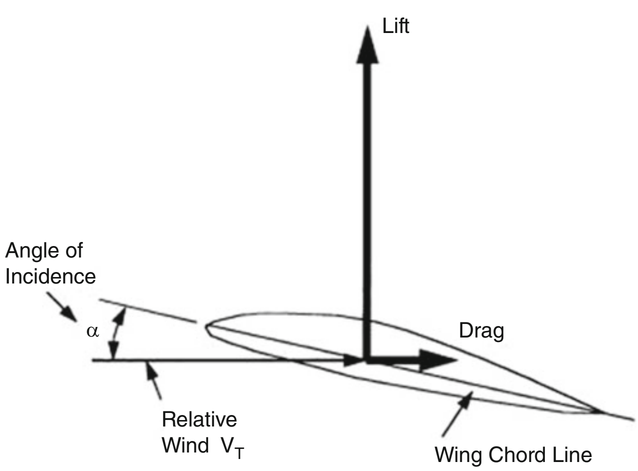

Fig. 3.3 Angle of incidence

3.2.3 Lift Coefficient and Drag Coefficient

Aerodynamic forces are dependent on the impact pressure, which, as explained in Chap. 2, is the pressure created by the change in kinetic energy of the airstream when it impacts on the surface. Aerodynamicists use the term dynamic pressure, Q, to denote the impact pressure which would result if air were incompressible.

$$\text{Dynamic pressure } Q = \frac{1}{2}\rho V_T{}^2 \tag{3.1}$$

where ρ is air density and V_T is air speed.

The aerodynamic lift force, L_W, acting on the wing is a function of the dynamic pressure, Q, the surface area of the wing, S, and a parameter which is dependent on the shape of the aerofoil section and the angle of incidence, α. This parameter is a non-dimensional coefficient, C_L, which is a function of the angle of incidence and is used to express the effectiveness of the aerofoil section in generating lift.

$$C_L = \frac{L_W}{\frac{1}{2}\rho V_T^2 S} \tag{3.2}$$

Thus

$$L_W = \frac{1}{2}\rho V_T{}^2 S C_L \tag{3.3}$$

The C_L versus α relationship is reasonably linear up to a certain value of angle of incidence when the airflow starts to break away from the upper surface and the lift falls off very rapidly – this is known as stalling. The slope of the C_L versus α relationship and the maximum value, $C_{L\,max}$, are dependent on the aerofoil section. $C_{L\,max}$ typically ranges from about 1.2 to 1.6. Maximum values of the angle of incidence before the onset of stalling range from 15 to 20° for conventional wing plans; for delta wing aircraft, the figure can be up to 30–35°. The C_L versus α relationship also changes as the aircraft speed approaches the speed of sound, and changes again at supersonic speeds.

Similarly, a non-dimensional characteristic called the *drag coefficient*, C_D, which is a function of the angle of incidence, α, is used to enable the drag characteristics of an aerofoil to be specified:

$$C_D = \frac{D_W}{\frac{1}{2}\rho V_T^2 S} \tag{3.4}$$

That is, drag force

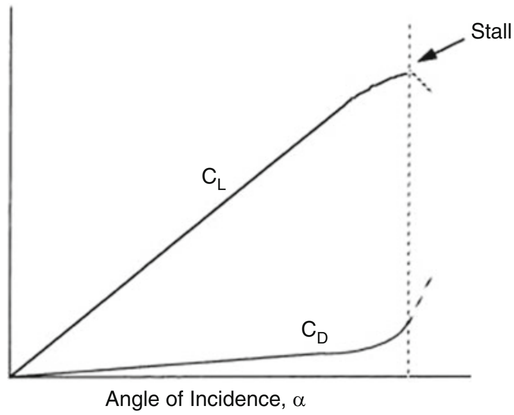

Fig. 3.4 C_L and C_D versus α

$$D_W = \frac{1}{2}\rho V_T^2 S C_D \tag{3.5}$$

The lift and drag characteristics of an aerofoil are related, the relationship being approximately

$$C_D = C_{DO} + k{C_L}^2 \tag{3.6}$$

where C_{DO} and k are constants for a particular aerofoil section.

Thus C_D increases rapidly at high values of C_L (and α). It also increases very rapidly indeed as the aircraft's speed approaches the speed of sound due to compressibility effects. The C_D versus α characteristics of a wing designed for supersonic operation are again very different at supersonic speeds compared with subsonic speeds.

Figure 3.4 shows the general shape for a typical subsonic aerofoil, of the relationship of C_L and C_D with α. These characteristics have been determined for a very wide range of standardised aerofoil sections. The selection of a particular aerofoil section in the aircraft design process is determined by the optimum combination of characteristics for the aircraft mission and range of operating height and speed conditions.

Matching the wing lift requirements over the flight envelope, for example, high lift at take-off and low drag at high speed, or increased lift for manoeuvring in combat, is achieved with the use of retractable leading edge flaps or slats and trailing edge flaps (see Fig. 3.5). These enable relatively large increases in C_L to be obtained with maximum values of C_{Lmax} between 3 and 4.

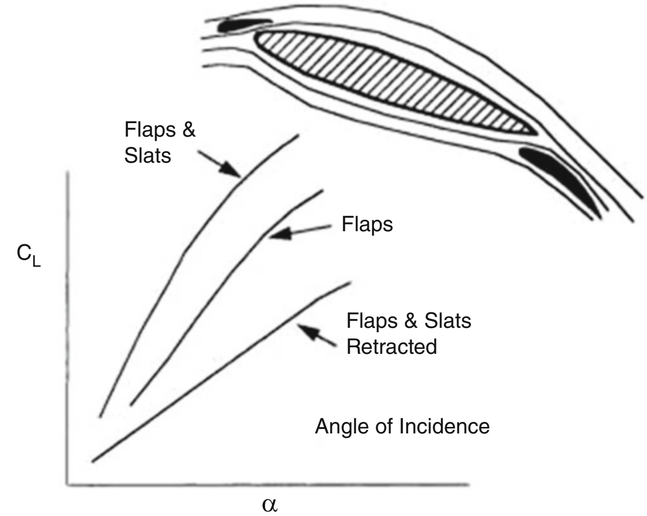

Fig. 3.5 Leading edge slats and trailing edge flaps

3.2.4 Illustrative Example on Basic Aerodynamics

A simple example of the application of these basic aerodynamic relationships is set out below. The object is to show how lift, incidence and manoeuvring capability can be estimated for various height and speed combinations so as to give an 'engineering feel' for the subject. The basic parameters for a hypothetical aircraft are as follows:

Aircraft mass, m 30,000 kg
Wing area, S 75 m^2
Maximum lift coeff, C_L max 1.2
Maximum angle of incidence, α_{max} 15°
C_L versus α relationship is assumed to be linear.
Air data: Air density, ρ_0, at sea level and standard temperature (15 °C) and pressure (1013.25 mbar) is 1.225 kg/m^3.
Air density, ρ, at 30,000 ft. (9144 m) is 0.4583 kg/m^3.
Question (i) What is the wing incidence, α, when flying straight and level at a speed of 80 m/s (160 knots approx.) at a height of 200 ft. in the approach to the airfield?
Question (ii) What is the corresponding wing incidence when flying straight and level at a speed of 200 m/s (400 knots approx.) at a height of 1000 ft.?
Note: Neglect change in density 0–1000 ft. for simplicity.
Question (iii) What is the maximum normal acceleration that can be achieved at a height of 30,000 ft. when flying at a speed of 225 m/s (450 knots)? Neglect compressibility effects and assume adequate thrust is available to counteract the increase in drag and maintain speed of 450 knots at α_{max}.

Case 1 Low Level/Low Speed

Dynamic pressure $Q = \frac{1}{2}\rho V_T{}^2 = 0.5 \times 1.225 \times 80^2 = 3920$ N/m^2

Wing lift $= QSC_L = 3920 \times 75 \times C_L$ N

Aircraft weight $= 30{,}000 \times 9.81$ N ($g = 9.81$ m/s^2)

Hence, $3920 \times 75 \times C_L = 30{,}000 \times 9.81$

and required $C_L = 1.0$.

C_L versus α is linear, hence

$$\frac{dC_L}{d\alpha} = \frac{C_{L\max}}{\alpha_{\max}} = \frac{1.2}{15}\,\text{degrees}^{-1}$$

$$C_L = \frac{dC_L}{d\alpha} \cdot \alpha$$

Hence,

$$\alpha = 1.0 \times \frac{15}{1.2} = 12.5°$$

Case 2 Low Level/High Speed

Lift is proportional to V_T^2, hence required incidence for straight and level flight at 200 m/s:

$$= \left(\frac{80}{200}\right)^2 \times 12.5 = 2°$$

Case 3 High Altitude/High Speed

Maximum achievable lift $= \frac{1}{2} \times 0.4583 \times 225^2 \times 75 \times 1.2 = 1044 \times 10^3$ N

Aircraft weight $= 294 \times 10^3$ N

Hence, lift available for manoeuvring $= 750 \times 10^3$ N

$$\begin{aligned}\text{Achievable normal acceleration}\\ &= \frac{\text{Normal force}}{\text{Aircraft mass}} = \frac{750 \times 10^3}{30,000}\\ &= 25\text{m/s}^2 = 2.5g\,(\text{approx.})\end{aligned}$$

3.2.5 Pitching Moment and Aerodynamic Centre

The *centre of pressure* is the point where the resultant lift and drag forces act and is the point where the moment of all the forces summed over the complete wing surface is zero. There will thus be a *pitching moment* exerted at any other point not at the centre of pressure. The centre of pressure varies with angle of incidence and for these reasons *aerodynamic centre* is now used as the reference point for defining the pitching moment acting on the wing. The aerodynamic centre of the wing is defined as the point about which the pitching moment does not change with angle of incidence (providing the velocity is constant). It should be noted that all aerofoils (except symmetrical ones) even at zero lift tend to pitch and experience a pitching moment or couple. The aerodynamic centre is generally around the quarter chord point of the wing (measured from the leading edge). At supersonic speeds, it tends to move aft to the half chord point. This pitching moment or couple experienced at zero lift, M_0, is again expressed in terms of a non-dimensional coefficient, pitching moment coefficient, C_{M_0}

$$C_{M_0} = \frac{M_0}{\frac{1}{2}\rho V_T{}^2 \text{Sc}} \tag{3.7}$$

where c is the *mean aerodynamic chord*, equal to wing area/wing span. Thus, pitching moment

$$M_0 = \frac{1}{2}\rho V_T^2 \text{Sc}\, C_{M_0} \tag{3.8}$$

3.2.6 Tailplane Contribution

The total pitching moment about the aircraft's centre of gravity (CG) and its relationship to the angle of incidence is of prime importance in determining the aircraft's stability. This will be discussed in the next section. However, it is appropriate at this stage to show how the resultant pitching moment about the CG is derived, particularly with a conventional aircraft configuration with a horizontal tailplane (refer to Fig. 3.6). The tailplane makes a major contribution to longitudinal stability and provides the necessary downward lift force to balance or trim the aircraft for straight and level

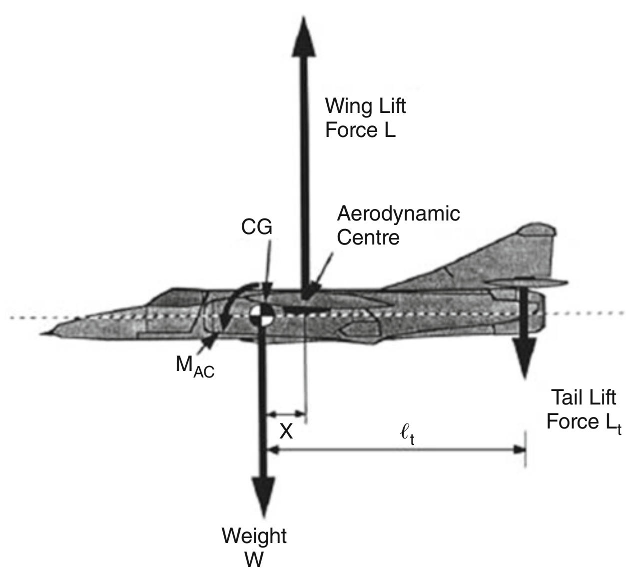

Fig. 3.6 Tailplane contribution

flight. The moment about the CG due to the tailplane lift balances the nose-down pitching moment due to the wing lift and the inherent wing pitching moment or couple, M_0. It should be noted that the trim lift exerted by the tailplane is in the opposite sense to the wing lift thereby reducing the total lift acting on the aircraft.

Resultant moment about CG, M, is given by

$$M = -L_W x - M_0 + L_t l_t \quad (3.9)$$

(nose-up momesnts are defined as positive).

Wing lift:

$$L_W = \frac{1}{2}\rho V_T{}^2 S C_L$$

Wing pitching moment:

$$M_0 = \frac{1}{2}\rho V_T{}^2 S c\, C_{M_0} \quad (3.10)$$

Tailplane lift:

$$L_t = k_t \frac{1}{2}\rho V_T{}^2 S_t C_{Lt} \quad (3.11)$$

where S_t is the tailplane area and C_{Lt} is the tailplane lift coefficient.

k_t is the ratio of the dynamic pressure at the tailplane to the freestream dynamic pressure and is known at the *tailplane efficiency factor*. This factor takes into account the effects of downwash from the airflow over the wings on the tailplane. The tailplane efficiency factor varies from 0.65 to 0.95 and depends on several factors such as the location of the tailplane with respect to the wing wake, etc.

Moment about CG due to tailplane lift is $k_t \frac{1}{2}\rho V_T{}^2 C_{Lt}(S_t l_t)$.

The term $(S_t\, l_t)$ is often called the *tailplane volume*.

Dividing both sides of Eq. (3.9) by $\frac{1}{2}\rho V_T{}^2 Sc$ yields

$$C_M = -\frac{x}{c} C_L - C_{M_0} + k_t \frac{(S_t l_t)}{Sc} C_{Lt} \quad (3.12)$$

The equation shows the respective contributions to the total pitching moment coefficient. However, the most important characteristic from the aerodynamic stability aspect is the variation of the overall pitching moment coefficient with incidence. (This will be clarified in the next section.) Figure 3.7 shows the variation with incidence of the wing and tailplane pitching moments and the combined pitching moment. It can be seen that the effect of the tailplane is to increase the negative slope of the overall pitching moment with incidence characteristics.

That is, $dC_M/d\alpha$ is more negative and this increases the aerodynamic stability.

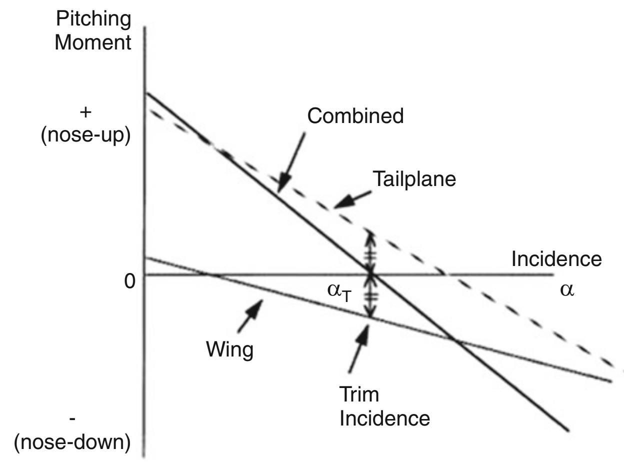

Fig. 3.7 Pitching moment versus incidence

3.3 Aircraft Stability

A stable system is one which returns to its original state if disturbed; a neutrally stable system remains in its disturbed state and an unstable system will diverge from its state on being subjected to the slightest disturbance. This is illustrated in Fig. 3.8, which shows a ball bearing placed on concave, flat and convex surfaces, respectively, as an analogous example of these three stability conditions. An aircraft is said to be stable if it tends to return to its original position after being subjected to a disturbance without any control action by the pilot. Figure 3.9a, b illustrates various degrees of stability, both statically and dynamically.

3.3.1 Longitudinal Stability

As already mentioned, to balance or trim the aircraft to achieve straight and level flight requires that the total pitching moment about the CG is zero and the total lift force equals the aircraft weight. However, to achieve static stability it is necessary that the total pitching moment coefficient, C_M, about the CG changes with angle of incidence, α, as shown in Fig. 3.10. The value of the angle of incidence at which the pitching moment coefficient about the CG is zero is known as the *trim angle of incidence*, α_T.

For values of angle of incidence less than α_T, the pitching moment coefficient is positive so the resulting pitching moment is in the nose-up sense and tends to restore the aircraft to the trim incidence angle, α_T. Conversely, for angles of incidence greater than α_T, the pitching moment coefficient is negative so the resultant nose-down moment tends to restore the aircraft to the trim incidence angle, α_T.

Thus $dC_M/d\alpha$ must be negative for longitudinal static stability and $C_M = 0$ at $\alpha = \alpha_T$.

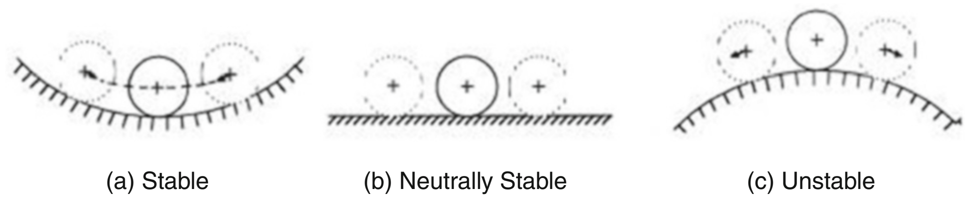

Fig. 3.8 Simple example of stability conditions

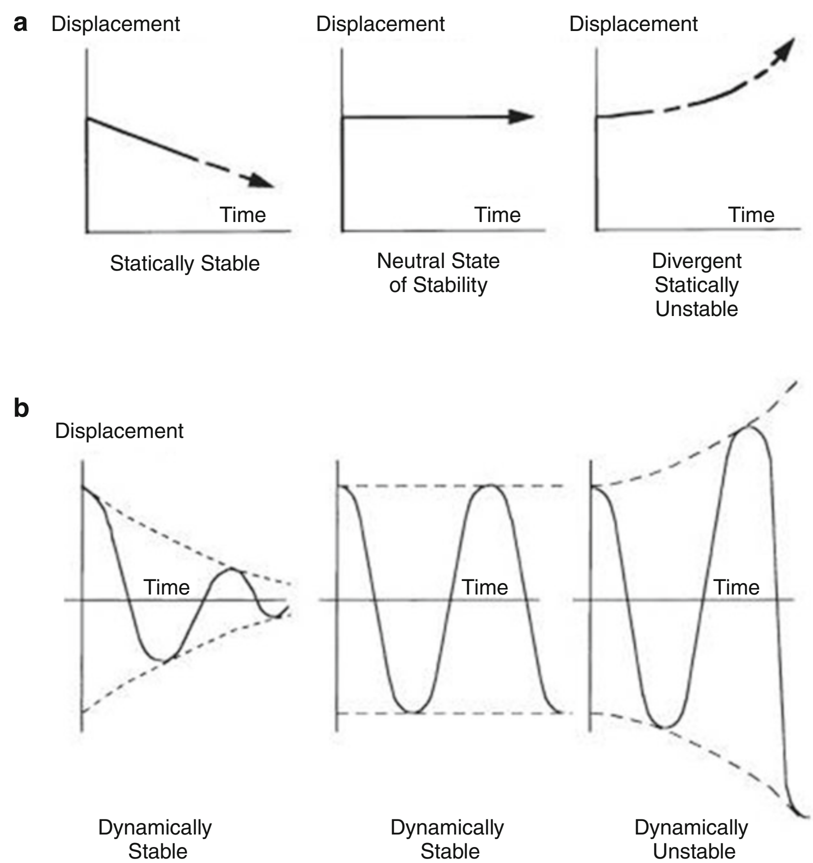

Fig. 3.9 (**a**) Static stability. (**b**) Dynamic stability

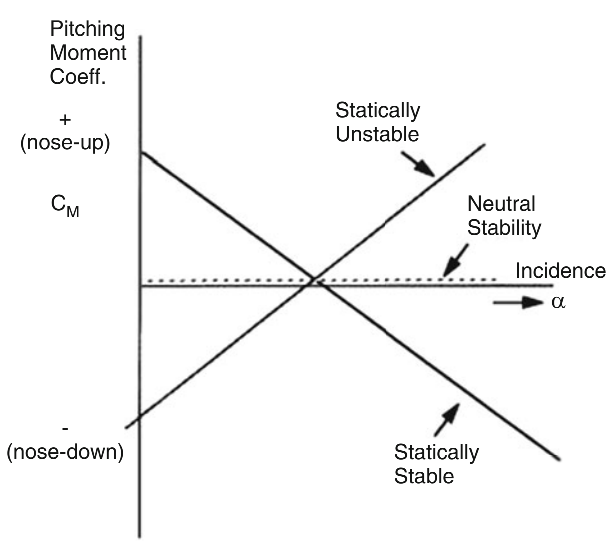

Fig. 3.10 C_M versus α

It should also be noted that the aircraft centre of gravity must be forward of the aerodynamic centre of the complete aircraft for static stability.

Static Margin and Neutral Point Movement of the CG rearwards towards the aerodynamic centre decreases the static stability.

The position of the CG where $dC_M/d\alpha = 0$ is known as the *neutral point* and corresponds to the position of the aerodynamic centre of the complete aircraft. The static margin of the aircraft is defined as the distance of the CG from the neutral point divided by the mean aerodynamic chord, *c*. This is positive when the CG is forward of the neutral point. Thus, the static margin is always positive for a stable aircraft. As an example, an aircraft with a static margin of 10% and a mean aerodynamic chord of, say, 4 m (13.3 ft) means that a rearward shift of the CG of more than 40 cm (16 in) would result in instability.

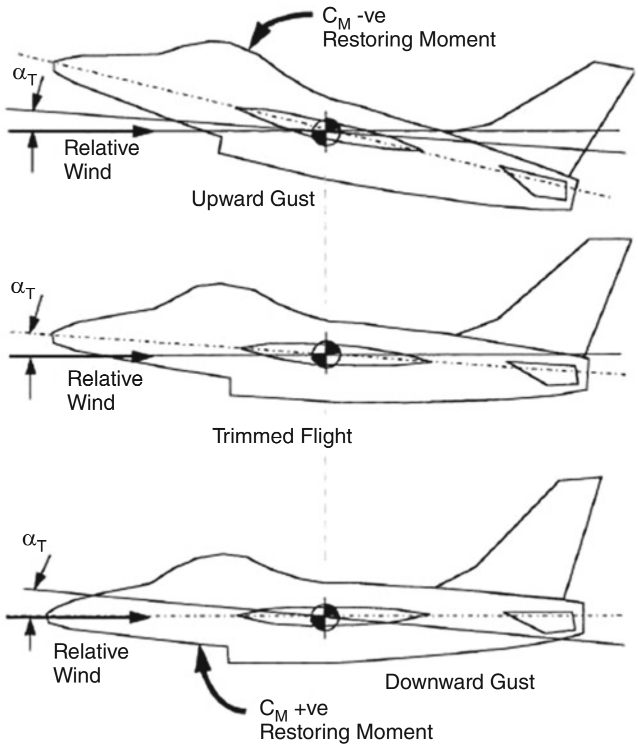

Fig. 3.11 Natural longitudinal stability

Figure 3.11 illustrates the restoring moments when a stable aircraft is disturbed, for instance, by being subjected to an upward or downward gust.

3.3.2 Aerodynamically Unstable Aircraft

Figure 3.12 shows an aerodynamically unstable aircraft with the CG aft of the aerodynamic centre. The tailplane trim lift is acting in the same sense as the wing lift and so is more aerodynamically efficient. The angle of incidence required for a given lift is lower thereby reducing the induced drag – the induced drag being proportional to the square of the angle of incidence ($C_D = C_{Do} + kC_L^2$, and C_L is approximately linear with α).

The tailplane volume ($S_t l_t$) can also be reduced further lowering the weight and drag and hence improving the performance, subject to other constraints such as rotation moment at take-off.

The pilot's speed of response to correct the tendency to divergence of an unstable aircraft is much too slow and the tailplane must be controlled automatically. The time for the divergence to double its amplitude following a disturbance can be of the order of 0.25 seconds or less on a modern high-agility fighter, which is aerodynamically unstable. The problem of flying an unstable aircraft has been compared to trying to steer a bicycle backwards (see Fig. 3.13).

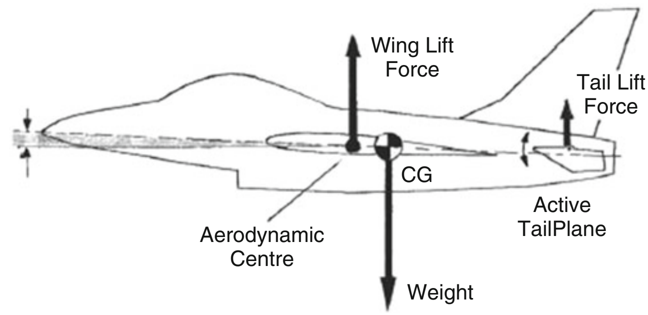

Fig. 3.12 Aerodynamically unstable aircraft

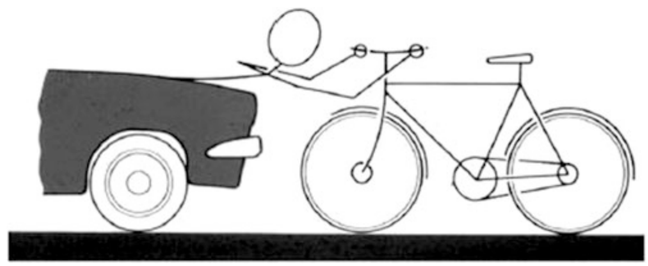

Fig. 3.13 Analogy of controlling aerodynamically unstable aircraft

Higher performance and increased agility can be obtained with an aerodynamically unstable aircraft and relying totally on an automatic stability system. The technology to implement such an automatic stability system with a manoeuvre command flight control system is now sufficiently mature to meet the very exacting safety and integrity requirements and system availability.

Such a system has become known as a 'fly-by-wire' flight control system because of its total dependence on electrical signal transmission and electronic computing, and will be covered in the next chapter. The difference between a negative tailplane lift and positive tailplane lift to trim the aircraft is strikingly illustrated in Fig. 3.14, which shows an aerodynamically stable aircraft (Tornado) flying in formation with an aerodynamically unstable aircraft (fly-by-wire Jaguar experimental aircraft).

3.3.3 Body Lift Contributions

It should be noted that lift forces are also generated by the fuselage. These fuselage (or body) lift forces are significant and they can also seriously affect both lateral and longitudinal aircraft stability. The engine casings in aircraft configurations with 'pod' type engine installations can also generate significant lift forces, which can again affect the aircraft stability.

3.4 Aircraft Dynamics

An aircraft has six degrees of freedom because its motion can involve both linear and angular movement with respect to three orthogonal axes. Deriving the dynamic response of the aircraft to disturbances or control surface movements first involves the generation of the differential equations which describe its motion mathematically. The solution of these equations then gives the response of the aircraft to a disturbance or control surface input. This enables the control that has to be exerted by the automatic flight control system to be examined on the basis of the aircraft's dynamic behaviour.

Fig. 3.14 Negative tailplane lift on Tornado. Positive tailplane lift on FBW Jaguar. (Photograph by Arthur Gibson provided by British Aerospace Defence Ltd.)

3.4.1 Aircraft Axes – Velocity and Acceleration Components

The aircraft motion is normally defined with respect to a set of orthogonal axes, known as body axes, which are fixed in the aircraft and move with it (see Fig. 3.15).

These axes are chosen for the following reasons:

(a) The equations of motion with respect to body axes are simpler.
(b) The aircraft motion can be readily measured with respect to body axes by robust motion sensors such as rate gyros and accelerometers, which are body mounted (i.e. 'strapped down').
(c) Body axes are natural ones for the pilot and are the axes along which the inertia forces during manoeuvres (e.g. the normal acceleration during turns) are sensed.
(d) The transformation of motion data with respect to body axes to fixed space axes is not difficult with modern processors. Broadly speaking, body axes are used in deriving the control dynamics and short-term behaviour of the aircraft. Space axes are more suitable for the longer-period guidance aspects in steering the aircraft to follow a particular flight path with respect to the Earth.

Referring to Fig. 3.15, the origin of the axes, O, is located at the centre of gravity (CG) of the aircraft with OX and OZ in the plane of symmetry of the aircraft (longitudinal plane), with OZ positive downwards and OY positive to starboard (right). The figure shows the longitudinal and lateral planes of the aircraft. A fixed frame of axes is assumed to be

Fig. 3.15 Aircraft axes and velocity components

AXIS	Linear Velocity Component	Angular Velocity Component
Forward or Roll Axis, 0X	Forward Velocity U	Roll Rate P
Sideslip or Pitch Axis, 0Y	Sideslip Velocity V	Pitch Rate q
Vertical or Yaw Axis, 0Z	Vertical Velocity W	Yaw Rate r

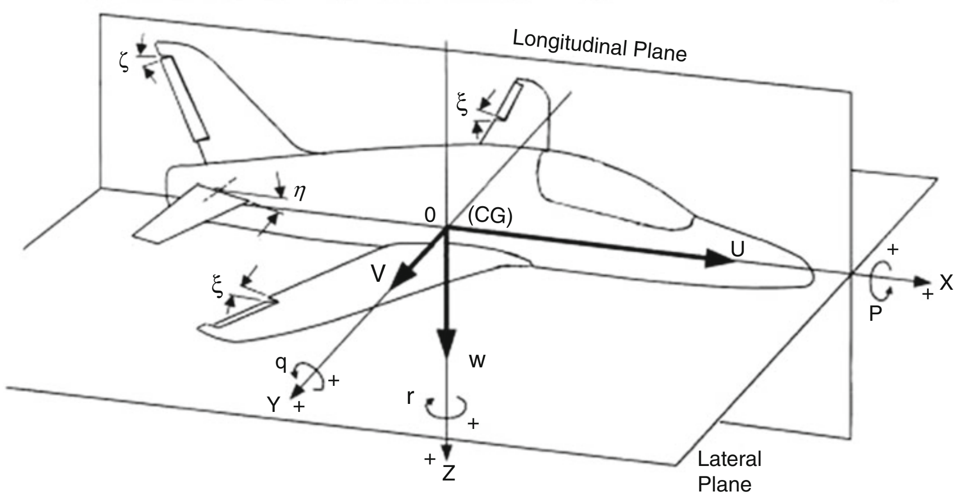

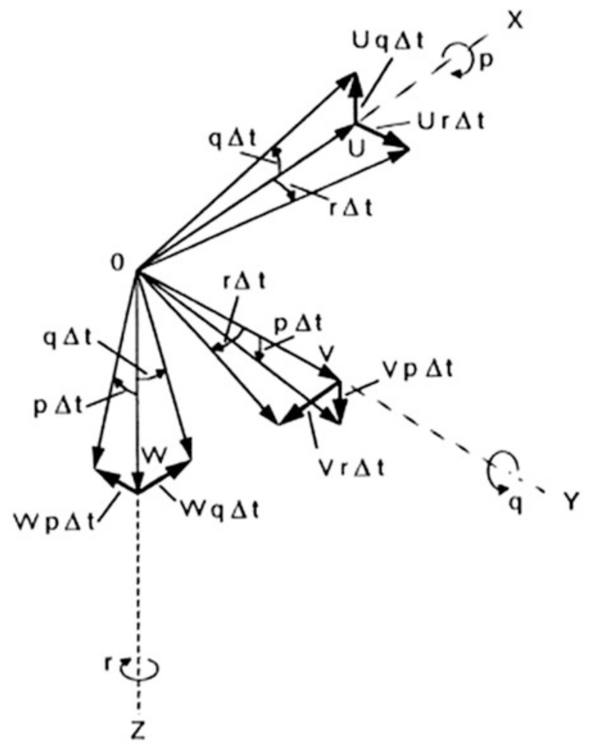

Fig. 3.16 Vector change in velocity components due to angular rotation

instantaneously coincident with the moving frame, and the velocity components of the aircraft CG along the OX, OY, OZ axes with respect to this fixed frame are the forward velocity, U, the sideslip velocity, V, and the vertical velocity, W, respectively. The corresponding angular rates of rotation of the body axes frame about OX, OY, OZ are the roll rate, p, the pitch rate, q, and the yaw rate, r, with respect to this fixed frame of axes. The derivation of the acceleration components when the aircraft's velocity vector is changing both in magnitude and direction is set out below as it is fundamental to deriving the equations of motion. Basically, the components are made up of centrifugal (strictly speaking centripetal) acceleration terms due to the changing direction of the velocity vector as well as the components due to its changing magnitude.

In Fig. 3.16, at time $t = 0$, the axes OX, OY, OZ are as shown in dotted lines. At time $t = \Delta t$, the angular rotations of the vector components are $p\Delta t$, $q\Delta t$, $r\Delta t$, respectively. The corresponding changes in the vectors are thus $-Uq\Delta t$, $Ur\Delta t$, $Vp\Delta t$, $-Vr\Delta t$, $-Wp\Delta t$, $Wq\Delta t$. The rates of change of these vectors, that is, the centripetal acceleration components, are thus: $-Uq$, Ur, Vp, $-Vr$, $-Wp$, Wq.

The changes in the velocity components due to the change in magnitude of the velocity vector are ΔU, ΔV, ΔW, respectively. The rates of change of these velocity components are $\Delta U/\Delta t$, $\Delta V/\Delta t$, $\Delta W/\Delta t$, which in the limit becomes dU/dt, dV/dt, dW/dt.

The linear acceleration components are thus:

$$\text{Acceleration along OX} = \dot{U} - Vr + Wq \tag{3.13}$$

$$\text{Acceleration along OY} = \dot{V} + Ur - Wp \tag{3.14}$$

$$\text{Acceleration along OZ} = \dot{W} - Uq + Vp \tag{3.15}$$

The angular acceleration components about OX, OY and OZ are $\dot{p}$, $\dot{q}$ and $\dot{r}$, respectively. The dot over the symbols denotes d/dt and is Newton's notation for a derivative. Thus, $\dot{U} = dU/dt$ and $\dot{p} = dp/dt$, etc.

The motion of the aircraft can then be derived by solving the differential equations of motion obtained by applying Newton's second law of motion in considering the forces and moments acting along and about the OX, OY and OZ axes, respectively. Namely, the rate of change of momentum is equal to the resultant force acting on the body, that is,

$$\text{Force} = \text{mass} \times \text{acceleration}$$

In the case of angular motion, this becomes:

$$\text{Moment (or torque)} = (\text{moment of inertia}) \times (\text{angular acceleration})$$

3.4.2 Euler Angles – Definition of Angles of Pitch, Bank and Yaw

The orientation of an aircraft with respect to a fixed inertial reference frame of axes is defined by the three Euler angles. Referring to Fig. 3.17, the aircraft is imagined as being oriented parallel to the fixed reference frame of axes. A series of rotations bring it to its present orientation:

(i) Clockwise rotation in the horizontal plane, through the yaw (or heading) angle ψ, followed by
(ii) A clockwise rotation about the pitch axis, through the pitch angle θ, followed by
(iii) A clockwise rotation about the roll axis, through the bank angle $\dot{\Phi}$

The order of these rotations is very important – a different orientation would result if the rotations were made in a different order.

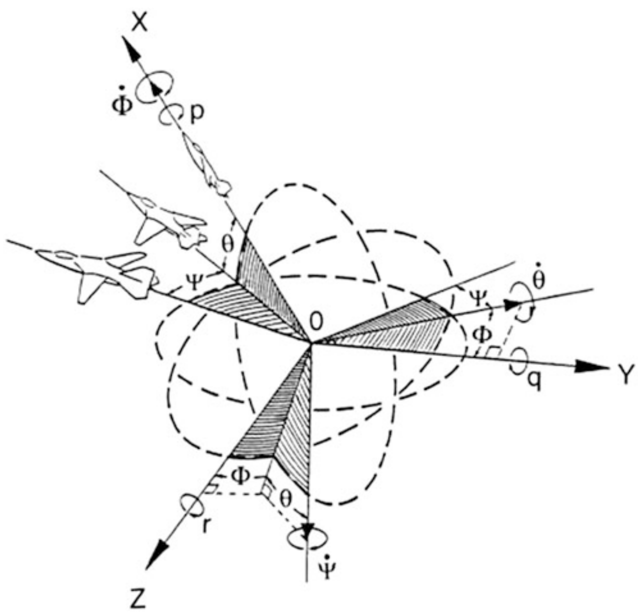

Fig. 3.17 Euler angles

The relationship between the angular rates of roll, pitch and yaw, p, q, r (which are measured by body mounted rate gyros) and the Euler angles, ψ, θ, Φ and the Euler angle rates $\dot{\psi}, \dot{\theta}, \dot{\Phi}$ are derived as follows:

Consider Euler bank angle rate, $\dot{\Phi}$

$$\text{Component of } \dot{\Phi} \text{ along } \begin{cases} \text{OX} = \dot{\Phi} \\ \text{OY} = 0 \\ \text{OZ} = 0 \end{cases}$$

Consider Euler pitch angle rate, $\dot{\theta}$

$$\text{Component of } \dot{\theta} \text{ along } \begin{cases} \text{OX} = 0 \\ \text{OY} = \dot{\theta}\cos\Phi \\ \text{OZ} = -\dot{\theta}\sin\Phi \end{cases}$$

Consider Euler yaw angle rate, $\dot{\psi}$

$$\text{Component of } \dot{\psi} \text{ along } \begin{cases} \text{OX} = -\dot{\Psi}\sin\theta \\ \text{OY} = \dot{\Psi}\cos\theta\sin\Phi \\ \text{OZ} = \dot{\Psi}\cos\theta\cos\Phi \end{cases}$$

Hence

$$p = \dot{\Phi} - \dot{\Psi}\sin\theta \tag{3.16}$$

$$q = \dot{\theta}\cos\Phi + \dot{\Psi}\cos\theta\sin\Phi \tag{3.17}$$

$$r = \dot{\Psi}\cos\theta\cos\Phi - \dot{\theta}\sin\Phi \tag{3.18}$$

It should be noted that these relationships will be referred to in Chap. 5, in the derivation of attitude from strap-down rate gyros.

3.4.3 Equations of Motion for Small Disturbances

The six equations of motion which describe an aircraft's linear and angular motion are non-linear differential equations. However, these can be linearised provided the disturbances from trimmed, straight and level flight are small. Thus in the steady state the aircraft is assumed to be moving in straight and level flight with uniform velocity and no angular rotation. That is, with no bank, yaw or sideslip and the axes OX and OZ lying in the vertical plane. The incremental changes in the velocity components of the CG along OX, OY, OZ in the disturbed motion are defined as u, v, w, respectively, and the incremental angular velocity components are p, q, r about OX, OY, OZ. The velocity components along OX, OY, OZ are thus (U_0 + u), v, (W_0 + w) in the disturbed motion where U_0 and W_0 are the velocity components along OX, OZ in steady flight ($V_0 = 0$, no sideslip). u, v, w, p, q, r are all small quantities compared with U_0 and W_0 and terms involving the products of these quantities can be neglected.

The acceleration components thus simplify to:

$$\dot{u} + W_0 q \tag{3.19}$$

$$\dot{v} - W_0 p + U_0 r \tag{3.20}$$

$$\dot{w} - U_0 q \tag{3.21}$$

The external forces acting on the aircraft are shown in Fig. 3.18 and comprise lift, drag, thrust and weight. These forces have components along OX, OY, OZ and can be separated into aerodynamic and propulsive force components and gravitational force components.

In the steady, straight and level trimmed flight condition, the resultant forces acting along OX, OY, OZ due to the lift, drag, thrust and weight are zero. The resultant moments about OX, OY, OZ are also zero. For small disturbances, it is therefore only necessary to consider the incremental changes in the forces and moments arising from the disturbance, in formulating the equations of motion (see Fig. 3.19). The incremental changes in the aerodynamic forces and moments are functions of the linear and angular velocity changes u, v, w and p, q, r, respectively. The resultant incremental changes in the aerodynamic forces during the disturbance along OX, OY, OZ are denoted by X_a, Y_a, Z_a, respectively.

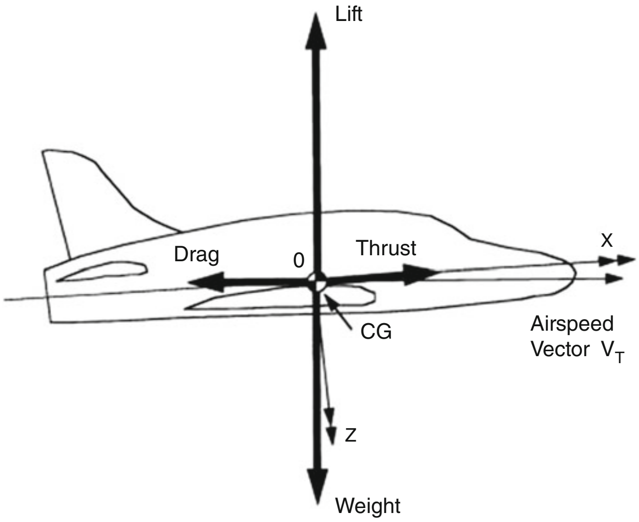

Fig. 3.18 External forces acting on aircraft

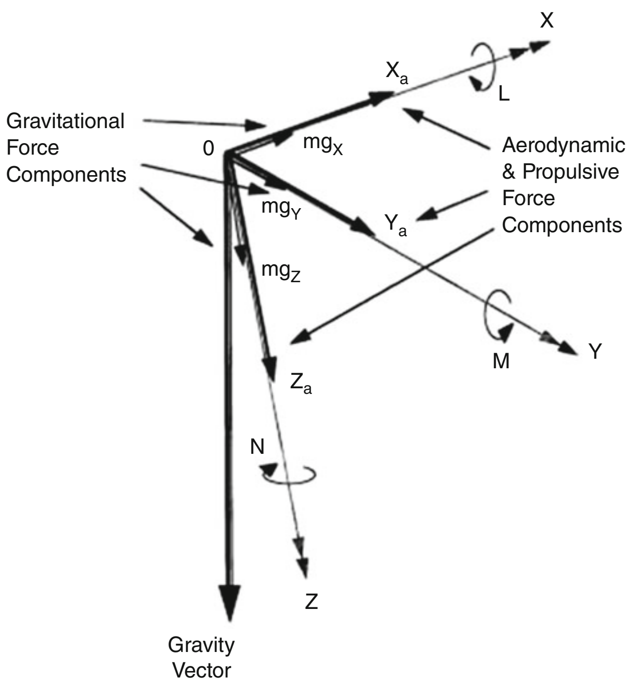

Fig. 3.19 Force components and moments

In the disturbed motion, the incremental changes in the components of the weight along OX, OY, OZ are approximately equal to $-mg\theta$, $mg\Phi$ and zero, respectively, assuming θ_0 is only a few degrees in magnitude.

From which the resultant incremental forces acting along OX, OY, OZ are

$$\text{along OX} = X_a - mg\theta$$
$$OY = Y_a + mg\Phi$$
$$OZ = Z_a$$

The equations of linear motion are thence derived from the relationship

$$\text{Force} = \text{mass} \times \text{acceleration}$$

$$X_a - mg\theta = m(\dot{u} + W_0 q) \tag{3.22}$$

$$Y_a + mg\Phi = m(\dot{v} - W_0 p + U_0 r) \tag{3.23}$$

$$Z_a = m(\dot{w} - U_0 q) \tag{3.24}$$

The resultant external moments acting on the aircraft due to the aerodynamic forces about OX, OY, OZ resulting from the disturbance are denoted by L, M, N, respectively.

Assuming principal axes are chosen for OX, OY, OZ so that the inertia product terms are zero.

The equations of angular motion are as follows:

$$L = I_x \dot{p} \tag{3.25}$$

$$M = I_y \dot{q} \tag{3.26}$$

$$N = I_z \dot{r} \tag{3.27}$$

It should be noted that the equations deriving the aircraft body rates in terms of Euler angles and Euler angle rates (refer to Sect. 3.4.2) can be simplified for small disturbances from straight and level flight. For small disturbances ψ, θ, Φ will all be small quantities of the first order and p, q, r (and $\dot{\psi}$, $\dot{\theta}$, $\dot{\Phi}$) can be taken to be small quantities of the first order. Thus neglecting second-order quantities, for small disturbances $p = \dot{\Phi}$, $q = \dot{\theta}$ and $r = \dot{\psi}$.

3.4.4 Aerodynamic Force and Moment Derivatives

The use of aerodynamic derivatives enables the incremental aerodynamic forces (X_a, Y_a, Z_a) and moments (L, M, N) to be expressed in terms of the force, or moment, derivatives multiplied by the appropriate incremental velocity change from the steady flight conditions. This linearises the equations of motion as the derivatives are assumed to be constant over small perturbations in the aircraft's motion. The equations of motion then become differential equations with constant coefficients and are much easier to analyse and solve. This assumption of constant derivatives is reasonable for small disturbances from a given flight condition. However, it is necessary to establish the variation in these derivatives over the range of height and speed and Mach number conditions over the entire flight envelope and mission.

These variations can be large and must be allowed for in estimating the responses.

The concept of the force and moment derivatives is based on estimating the change resulting from a change in an individual variable with all the other variables held constant. The resultant change is then the sum of all the changes resulting from the individual variable changes.

Thus if a quantity, F, is a function of several independent variables $x_1, x_2, x_3,..., x_n$, that is, $F = f(x_1, x_2, x_3,..., x_n)$, then the resultant change, ΔF, is given by

$$\Delta F = \frac{\partial F}{\partial x_1} \cdot \Delta x_1 + \frac{\partial F}{\partial x_2} \cdot \Delta x_2 + \frac{\partial F}{\partial x_3} \cdot \Delta x_3 \ldots + \frac{\partial F}{\partial x_n} \cdot \Delta x_n$$

$\partial F/\partial x_1$, $\partial F/\partial x_2$, $\partial F/\partial x_3$,..., $\partial F/\partial x_n$ are the partial derivatives of F with respect to $x_1, x_2, x_3,...,x_n$.

The notation adopted for derivatives is to indicate the partial derivative variable by means of a suffix. Thus

$$\frac{\partial F}{\partial x_1} = F_{x_1}, \quad \frac{\partial F}{\partial x_2} = F_{x_2}, \quad \frac{\partial F}{\partial x_3} = F_{x_3} \ldots \frac{\partial F}{\partial x_n} = F_{x_n}$$

hence

$$\Delta F = F_{x_1}\Delta x_1 + F_{x_2}\Delta x_2 + F_{x_3}\Delta x_3 \ldots + F_{x_n}\Delta x_n$$

The aerodynamic forces and moments acting on the aircraft are functions of the linear and angular velocity components u, v, w, p, q, r of the aircraft (all small quantities of the first order).

The forces acting along OX, OY, OZ are X, Y, Z, respectively, and the corresponding moments about OX, OY and OZ are L, M and N. The derivatives of these forces and moments due to a change in a particular variable are thus denoted by the appropriate suffix, for example X_u, X_w, Y_v, Z_w, L_p, M_q, N_r, N_v, corresponding forces and moments being $X_u u$, $X_w w$, $Y_v v$, $Z_w w$, $L_p p$, $M_q q$, $N_r r$, $N_v v$, etc. It should be noted that some text books and reference books use a 'dressing' (°) over the top of the symbol to denote a derivative, the (°) indicating the value is expressed in ordinary SI (*Le Systèm Internationale d'Unités*) units, for example, $\circ X_u$, $\circ Y_v$, $\circ M_q$.

There are also forces and moments exerted due to the movement of the control surfaces from their trimmed position. Thus in the case of controlling the aircraft's motion in the longitudinal plane by movement of the tailplane (or elevator) from its trimmed position by an amount, η, the corresponding force exerted along the OZ axis would be $Z_\eta \eta$ and the corresponding moment exerted about the OY axis would be $M_\eta\, \eta$.

Because the disturbances are small, there is no cross-coupling between longitudinal motion and lateral motion. For example, a small change in forward speed or angle of pitch does not produce any side force or rolling or yawing moment. Similarly, a disturbance such as sideslip, rate of roll and rate of yaw produces only second-order forces or moments in the longitudinal plane. Thus the six equations of motion can be split into two groups of three equations.

(a) Longitudinal equations of motion involving linear motion along the OX and OZ axes and angular motion about the OY axis.
(b) Lateral equations of motion involving linear motion along the OY axis and angular motion about the OX and OZ axes.

Thus each group of three equations can be solved separately without having to deal with the full set of six equations.

3.4.4.1 Longitudinal Motion Derivatives

These comprise the forward and vertical force derivatives and pitching moment derivatives arising from the changes in forward velocity, u, vertical velocity, w, rate of pitch, q, and rate of change of vertical velocity, $\dot{w}$.

The main longitudinal derivatives due to u, v, q and w are shown below.

Forward velocity, u

$$\begin{cases} \text{Forward force derivative } X_u \\ \text{Vertical force derivative } Z_u \end{cases}$$

Vertical velocity, w

$$\begin{cases} \text{Forward force derivative } X_w \\ \text{Vertical force derivative } Z_w \\ \text{Pitching moment derivative } M_w \end{cases}$$

Rate of pitch, q

$$\begin{cases} \text{Vertical force derivative } Z_q \\ \text{Pitching moment derivative } M_q \end{cases}$$

Rate of change of vertical velocity, $\dot{w}$

$$\begin{cases} \text{Vertical force derivative } Z_{\dot{w}} \\ \text{Pitching moment derivative } M_{\dot{w}} \end{cases}$$

***Force Derivatives Due to Forward Velocity* X_u, Z_u *and Vertical Velocity* X_w, Z_w** The changes in the forward velocity, u, and vertical velocity, w, occurring during the disturbance from steady flight result in changes in the incidence angle, α, and air speed, V_T. These changes in incidence and air speed result in changes in the lift and drag forces. The derivatives depend upon the aircraft's lift and drag coefficients and the rate of change of these coefficients with incidence and speed.

The forward force derivative X_u due to the change in forward velocity, u, and the forward force derivative, X_w, due to the change in vertical velocity, arise from the change in drag resulting from the changes in airspeed and incidence, respectively. The resulting forward force components are $X_u u$ and $X_w w$. The *vertical force derivative* Z_u, due to the forward velocity change, u, and the *vertical force derivative* Z_w, due to the vertical velocity change, w, arise from the change in lift due to the changes in airspeed and incidence, respectively. The resulting vertical force components are equal to $Z_u u$ and $Z_w w$.

***Pitching Moment Derivative Due to Vertical Velocity,* M**

$\mathbf{M_w}$ The change in incidence resulting from the change in the vertical velocity, w, causes the pitching moment about the CG to change accordingly. The resulting pitching moment is equal to $M_w w$ where M_w is the pitching moment derivative due to the change in vertical velocity, w. This derivative is very important from the aspect of the aircraft's longitudinal stability.

It should be noted that there is also a pitching moment derivative M_u due to the change in forward velocity, u, but this derivative is generally small compared with M_w.

***Force and Moment Derivatives Due to Rate of Pitch* $\mathbf{Z_q}$, $\mathbf{M_q}$** These derivatives arise from the effective change in the tailplane angle of incidence due to the normal velocity component of the tailplane. This results from the aircraft's angular rate of pitch, q, about the CG and the distance of the tailplane from the CG, l_t (see Fig. 3.20). This normal velocity component is equal to $l_t q$ and the effective change in the tailplane angle of incidence is equal to $l_t q/V_T$. This incidence change results in a lift force acting on the tailplane, which is multiplied by the tail moment arm, l_t, to give a significant damping moment to oppose the rate of rotation in pitch.

The vertical force (acting on the tailplane) is equal to $Z_q q$ where Z_q is the vertical force derivative due to rate of pitch, q. The resultant pitching moment about the CG is equal to $M_q q$ where M_q is the pitching moment derivative due to the rate of pitch, q. The M_q derivative has a direct effect on the damping of the aircraft's response to a disturbance or control input and is a very important derivative from this aspect. The use of auto-stabilisation systems to artificially augment this derivative will be covered later in this chapter.

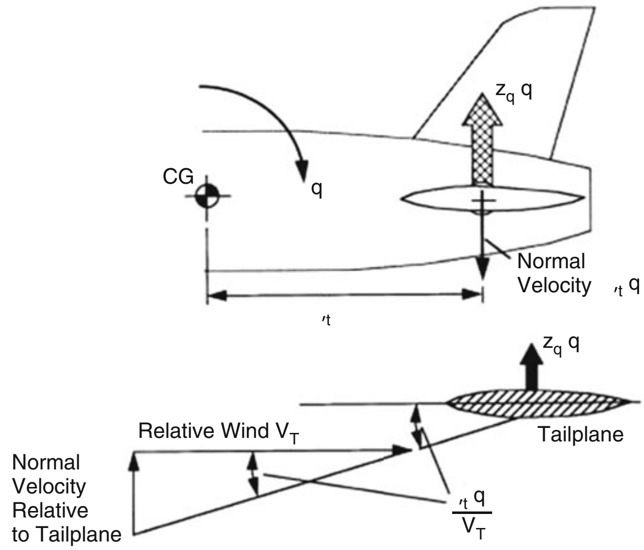

Fig. 3.20 Damping moment due to pitch rate

***Force and Moment Derivatives Due to the Rate of Change of Vertical Velocity* $\mathbf{Z_{\dot{w}}}$, $\mathbf{M_{\dot{w}}}$** These force and moment derivatives result from the lag in the downwash from the wing acting on the tailplane and are proportional to the rate of change of downwash angle with wing incidence. The resulting vertical force component is equal to $Z_{\dot{w}}\dot{w}$ and the resulting pitching moment is equal to $M_{\dot{w}}\dot{w}$ where $Z_{\dot{w}}$ is the vertical force derivative due to rate of change of vertical velocity, $\dot{w}$, and $M_{\dot{w}}$ is the pitching moment derivative due to the rate of change of vertical velocity, $\dot{w}$.

***Control Derivatives* $\mathbf{Z_\eta}$, $\mathbf{M_\eta}$** Control of the aircraft in the longitudinal plane is achieved by the angular movement of the tailplane (or elevator) by the pilot. The lift force acting on the tailplane as a result of the change in tailplane incidence creates a pitching moment about the aircraft's CG because of the tail moment arm. The pitching moment is proportional to the tailplane (or elevator) angular movement. The vertical force resulting from the tailplane (or elevator) movement is equal to $Z_\eta \eta$ where Z_η is the vertical force derivative due to the angular movement of the tailplane, η, from its steady, trimmed flight position. The pitching moment is equal to $M_\eta \eta$ when M_η is the pitching moment derivative due to the change in tailplane angle, η.

Longitudinal Forces and Moments

The main forces and moments acting along and about the OX, OY, OZ axes affecting longitudinal motion are set out below:

$$X_a = X_u u + X_w w \tag{3.28}$$

$$Z_a = Z_u u + Z_w w + Z_{\dot{w}} \dot{w} + Z_q q + Z_\eta \eta \quad (3.29)$$

$$M = M_w w + M_q q + M_{\dot{w}} \dot{w} + M_\eta \eta \quad (3.30)$$

3.4.4.2 Lateral Motion Derivatives

Changes in the sideslip velocity, v, rate of roll, p, and rate of yaw, r, following a disturbance from steady flight produces both rolling and yawing moments. This causes motion about the roll axis to cross-couple into the yaw axis and vice versa. The sideslip velocity also results in a side force being generated. The main lateral motion derivatives due to v, p and r are shown below:

Sideslip velocity v

- Side force derivative Y_v
- Yawing moment derivative N_v
- Rolling moment derivative L_v

Rate of roll, p

- Rolling moment derivative L_p
- Yawing moment derivative N_p

Rate of yaw, r

- Yawing moment derivative N_r
- Rolling moment derivative L_r

***Side Force Derivative Due to Sideslip Velocity* $\mathbf{Y_v}$** The change in sideslip velocity, v, during a disturbance changes the incidence angle, β, of the aircraft's velocity vector, V_T, (or relative wind) to the vertical surfaces of the aircraft comprising the fin and fuselage sides (see Fig. 3.21). The change in incidence angle v/V_T results in a sideways lifting force being generated by these surfaces. The net side force from the fuselage and fin combined is equal to $Y_v v$ where Y_v is the side force derivative due to the sideslip velocity.

***Yawing Moment Derivative Due to Sideslip Velocity* $\mathbf{N_v}$** The side force on the fin due to the incidence, β, resulting from the sideslip velocity, v, creates a yawing moment about the CG, which tends to align the aircraft with the relative wind in a similar manner to a weathercock (refer to Fig. 3.21).

The main function of the fin is to provide this directional stability (often referred to as weathercock stability). This yawing moment is proportional to the sideslip velocity and is dependent on the dynamic pressure, fin area, fin lift coefficient and the fin moment arm, the latter being the distance between the aerodynamic centre of the fin and the yaw axis through the CG. However, the aerodynamic lateral forces acting on the fuselage during sideslipping also produce a yawing moment which opposes the yawing moment due to the fin and so is destabilising. The net yawing moment due to sideslip is thus dependent on the combined contribution of the fin and fuselage. The fin area and moment arm, known as the *fin volume*, is thus sized to provide good directional stability under all conditions and subject to other constraints such as engine failure in the case of a multi-engine aircraft.

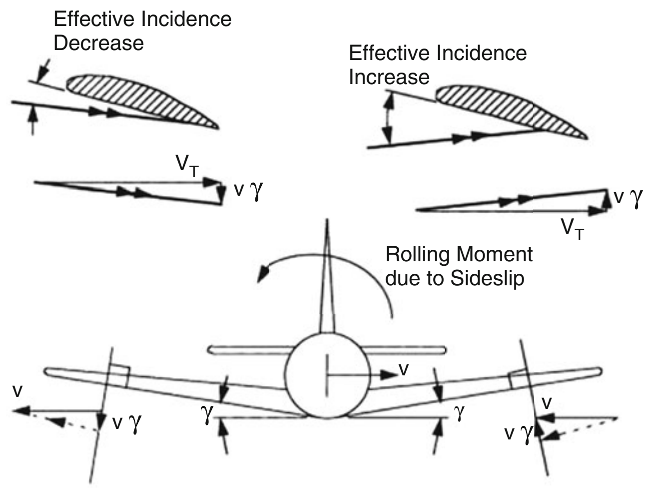

Fig. 3.21 Lateral forces

The yawing moment due to sideslip velocity is equal to $N_v v$ where N_v is the yawing moment derivative due to sideslip velocity.

***Rolling Moment Derivative Due to Sideslip Velocity* $\mathbf{L_v}$** When the aircraft experiences a sideslip velocity, the effect of wing dihedral is for this sideslip velocity to increase the incidence on one wing and reduce it on the other (see Fig. 3.22). Thus if one wing tends to drop whilst sideslipping, there is a rolling moment created which tends to level the wings.

The effect of wing sweepback is also to give a differential incidence change on the wings and a rolling moment is generated, even if the dihedral is zero. There is also a contribution to the rolling moment due to sideslip from the fin. This is because of the resulting lift force acting on the fin and the height of the aerodynamic centre of the fin above the roll axis. There is also a contribution from the fuselage due to flow effects round the fuselage, which affect the local wing incidence. These are beneficial in the case of a high wing and detrimental in the case of low wing. It is in fact necessary to incorporate considerably greater dihedral for a low wing than that required for a high wing location. The rolling moment derivative due to sideslip is denoted by L_v and the rolling moment due to sideslip is equal to $L_v v$.

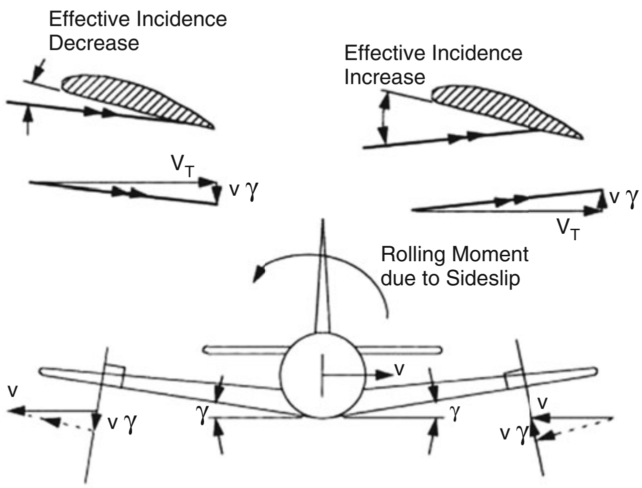

Fig. 3.22 Effect of dihedral and sideslip

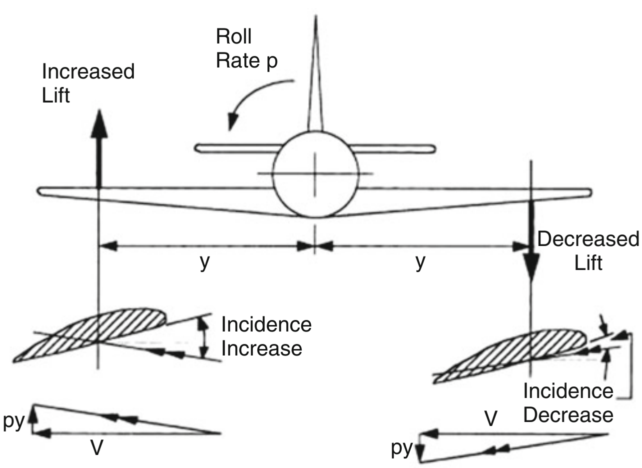

Fig. 3.23 Rolling moment due to rate of roll

Rolling Moment Derivative Due to Rate of Roll $\mathbf{L}_p$ When the aircraft is rolling, the angular velocity causes each section of wing across the span to experience a tangential velocity component which is directly proportional to its distance from the centre. Referring to Fig. 3.23, it can be seen that one section of wing experiences an increase in incidence whilst the corresponding section on the other wing experiences a decrease. The lift force exerted on one wing is thus increased whilst that on the other wing is decreased and a rolling moment is thus generated. The rolling moment due to the rate of roll, p, acts in the opposite sense to the direction of rolling and is equal to $L_p p$ where L_p is the rolling moment derivative due to rate of roll.

Yawing Moment Derivative Due to Rate of Roll $\mathbf{N}_p$ The rate of roll which increases the lift on the outer part of one wing and reduces it on the other also creates a differential drag effect. The increase in lift is accompanied by an increase in drag in the forward direction and the decrease in lift on the other wing by a corresponding reduction in drag. A yawing moment is thus produced by the rate of roll, p, which is equal to $N_p p$ where N_p is the yawing moment derivative due to rate of roll.

Yawing Moment Derivative Due to Rate of Yaw $\mathbf{N}_r$ The rate of yaw, r, produces a tangential velocity component equal to $l_f\, r$ where l_f is the distance between the aerodynamic centre of the fin and the yaw axis through the CG. The resulting change in the effective fin incidence angle, $l_f\, r/V_T$, produces a lift force which exerts a damping moment about the CG opposing the rate of yaw. The yawing moment due to the rate of yaw is equal to $N_r r$ where N_r is the yawing moment derivative due to rate of yaw.

Rolling Moment Derivative Due to Rate of Yaw $\mathbf{L}_r$ When the aircraft yaws, the angular velocity causes one wing to experience an increase in velocity relative to the airstream and the other wing a decrease. The lift on the leading wing is thus increased and the trailing wing decreased thereby producing a rolling moment. The rolling moment derivative due to rate of yaw is denoted by L_r and the rolling moment due to rate of yaw is equal to $L_r r$.

Lateral Control Derivatives Due to Ailerons and Rudder The ailerons and rudder are illustrated in Fig. 3.15. The angle through which the ailerons are deflected differentially from their position in steady, trimmed flight is denoted by ξ and the angle the rudder is deflected from the position in steady, trimmed flight is denoted by ζ.

Differential movement of the ailerons provides the prime means of lateral control by exerting a controlled rolling moment to bank the aircraft to turn; this will be covered later in this chapter.

Rolling Moment Derivative Due to Aileron Deflection L_ξ The effect of the differential deflection of the ailerons from their steady, trimmed flight position, ξ, is to increase the lift on one wing and reduce it on the other thereby creating a rolling moment. The rolling moment due to the aileron deflection is equal to $L_\xi \xi$ where L_ξ is the rolling moment derivative due to aileron deflection.

Yawing Moment Derivative Due to Aileron Deflection $\mathbf{N}_\xi$ The differential lift referred to above is also accompanied by a differential drag on the wings which results in a yawing moment being exerted. The yawing moment due to the aileron deflection is equal to $N_\xi \xi$ where N_ξ is the yawing moment derivative due to aileron deflection.

Deflection of the rudder creates a lateral force and yawing moment to counteract sideslipping motion and the yawing moment due to the movement of the ailerons. (The control function of the rudder will be covered in more detail later in this chapter).

Side Force Derivative Due to Rudder Deflection $\mathbf{Y}_\zeta$ The sideways lift force acting on the fin due to the deflection of the rudder, ζ, from its steady, trimmed flight position is equal to $Y_\zeta \zeta$ where Y_ζ is the side force derivative due to rudder deflection.

Yawing Moment Derivative Due to Rudder Deflection $\underline{N_\zeta}$ The yawing moment exerted by the rudder is equal to $N_\zeta \zeta$ where N_ζ is the yawing moment derivative due to the deflection of the rudder from its steady, trimmed flight position.

Lateral Forces and Moments

The main sideways force, Y_a, the rolling moment, L, and the yawing moment, N, resulting from changes in the sideslip velocity, v, rate of roll, p, and rate of yaw, r, from the steady flight condition are set out below.

$$Y_a = Y_v v + Y_\zeta \zeta \tag{3.31}$$

$$L = L_v v + L_p p + L_r r + L_\xi \xi + L_\zeta \zeta \tag{3.32}$$

$$N = N_v v + N_p p + N_r r + N_\xi \xi + N_\zeta \zeta \tag{3.33}$$

Normalisation of Derivatives

It should be noted that the derivatives are sometimes normalised and non-dimensionalised by dividing by the appropriate quantities – air density, airspeed, mean aerodynamic chord, wing span, etc. The appropriate quantities depend on whether it is a force/velocity derivative or a moment/angular rate derivative, etc. The equations of motion are also sometimes non-dimensionalised by dividing by the aircraft mass, moments of inertia, etc.

This enables aircraft responses to be compared independently of speed, air density, size, mass, inertia, etc. This stage has been omitted in this book for simplicity.

Readers wishing to find out more about non-dimensionalised derivatives and equations are referred to 'Further Reading' at the end of this chapter.

3.4.5 Equations of Longitudinal and Lateral Motion

Equations (3.28), (3.29) and (3.30) for X_a, Z_a and M can be substituted in the equations of motion (3.22), (3.24) and (3.26), respectively.

The equations of longitudinal motion for small disturbances then become:

$$X_u u + X_w w - mg\theta = m(\dot{u} + W_0 q) \tag{3.34}$$

$$Z_u u + Z_w w + Z_{\dot{w}} \dot{w} + Z_q q + Z_\eta \eta = m(\dot{w} - U_0 q)) \tag{3.35}$$

$$M_w w + M_q q + M_{\dot{w}} \dot{w} + M_\eta \eta = I_y \dot{q} \tag{3.36}$$

Equations (3.31), (3.32) and (3.33) for Y_a, L and N can similarly be substituted in the equations of motion (3.23), (3.25) and (3.27), respectively. The equations of lateral motion for small disturbances then become:

$$Y_v v + Y_\zeta \zeta + mg\Phi = m(\dot{v} - W_0 p + U_0 r) \tag{3.37}$$

$$L_v v + L_p p + L_r r + L_\zeta \zeta + L_\xi \xi = I_x \dot{p} \tag{3.38}$$

$$N_v v + N_p p + N_r r + N_\zeta \zeta + N_\xi \xi = I_z \dot{r} \tag{3.39}$$

These equations can be re-arranged as a set of first-order differential equations to express the first derivative of each variable as a linear equation relating all the variables in the set. The longitudinal equations have been simplified for clarity by omitting the $Z_q q$, $Z_{\dot{w}} \dot{w}$ and $M_{\dot{w}} \dot{w}$ terms. Hence, from Eqs. (3.34), (3.35) and (3.36) and noting that $q = \dot{\theta}$ for small disturbances,

$$\left.\begin{aligned}
\dot{u} &= \frac{X_u}{m} u + \frac{X_w}{m} w - W_0 q - g\theta \\
\dot{w} &= \frac{z_u}{m} u + \frac{z_w}{m} w + U_0 q \quad + \frac{Z_\eta}{m} \eta \\
\dot{q} &= \frac{M_w}{I_y} w + \frac{M_q}{I_y} q \quad + \frac{M_\eta}{I_y} \eta \\
\dot{\theta} &= q
\end{aligned}\right\} \tag{3.40}$$

Similarly, from Eqs. (3.37), (3.38) and (3.39) and noting that $p = \dot{\Phi}$ for small disturbances,

$$\left.\begin{aligned}
\dot{v} &= \frac{Y_v}{m} v + W_0 p - U_0 r + g\Phi + \frac{Y_\zeta}{m} \zeta \\
\dot{p} &= \frac{L_v}{I_x} v + \frac{L_p}{I_x} p + \frac{L_r}{I_x} r \quad + \frac{L_\zeta}{I_x} \zeta + \frac{L_\xi}{I_x} \xi \\
\dot{r} &= \frac{N_v}{I_z} v + \frac{N_p}{I_z} p + \frac{N_r}{I_z} r \quad + \frac{N_\zeta}{I_z} \zeta + \frac{N_\xi}{I_z} \xi \\
\dot{\Phi} &= p
\end{aligned}\right\} \tag{3.41}$$

These equations can be solved in a step-by-step, or iterative, manner by continuously computing the first derivative at each increment of time and using it to derive the change in the variables over the time increment and hence update the value at the next time increment.

As a simplified example, suppose the first-order equations relating three variables x, y, z are as follows:

$$\dot{x} = a_1 x + b_1 y + c_1 z$$
$$\dot{y} = a_2 x + b_2 y + c_2 z$$
$$\dot{z} = a_3 x + b_3 y + c_3 z$$

Let Δt = time increment, value of x at time $n\Delta t$ be denoted by x_n and value of □ at time $n\Delta t$ be denoted by □$_n$.

Value of x at time $(n + 1)\Delta t$, that is $x_{(n+1)}$, is given by

$$x_{(n+1)} = x_n + \dot{x}_n \cdot \Delta t$$

(assuming Δt is chosen as a suitably small time increment).

Hence

$$x_{(n+1)} = x_n + (a_1 x_n + b_1 y_n + c_1 z_n)\Delta t$$

a form suitable for implementation in a digital computer.

These equations can be expressed in the matrix format

$$\begin{bmatrix} \dot{x} \\ \dot{y} \\ \dot{z} \end{bmatrix} = \begin{bmatrix} a_1 & b_1 & c_1 \\ a_2 & b_2 & c_2 \\ a_3 & b_3 & c_3 \end{bmatrix} \begin{bmatrix} x \\ y \\ z \end{bmatrix}$$

Similarly, Eqs. (3.40) and (3.41) can be expressed as follows:

$$\begin{bmatrix} \dot{u} \\ \dot{w} \\ \dot{q} \\ \dot{\theta} \end{bmatrix} = \begin{bmatrix} \frac{X_u}{m} & \frac{X_w}{m} & -W_0 & -g \\ \frac{Z_u}{m} & \frac{Z_w}{m} & U_0 & 0 \\ 0 & \frac{M_w}{I_y} & \frac{M_q}{I_y} & 0 \\ 0 & 0 & 1 & 0 \end{bmatrix} \begin{bmatrix} u \\ w \\ q \\ \theta \end{bmatrix} + \begin{bmatrix} 0 \\ \frac{z_\eta}{m} \\ \frac{M_\eta}{I_y} \\ 0 \end{bmatrix} [\eta] \quad (3.42)$$

$$\begin{bmatrix} \dot{v} \\ \dot{p} \\ \dot{r} \\ \dot{\Phi} \end{bmatrix} = \begin{bmatrix} \frac{Y_v}{m} & W_0 & -U_0 & g \\ \frac{L_v}{I_x} & \frac{L_p}{I_x} & \frac{L_r}{I_x} & 0 \\ \frac{N_v}{I_z} & \frac{N_p}{I_z} & \frac{N_r}{I_z} & 0 \\ 0 & 1 & 0 & 0 \end{bmatrix} \begin{bmatrix} v \\ p \\ r \\ \Phi \end{bmatrix} + \begin{bmatrix} \frac{Y_\zeta}{m} & 0 \\ \frac{L_\zeta}{I_x} & \frac{L_\xi}{I_x} \\ \frac{N_\zeta}{I_z} & \frac{N_\xi}{I_z} \\ 0 & 0 \end{bmatrix} \begin{bmatrix} \zeta \\ \xi \end{bmatrix} \quad (3.43)$$

The use of a matrix format for the equations of motion gives much more compact expressions and enables the equations to be manipulated using matrix algebra.

The equations can be expressed in the general form

$$\dot{\mathbf{X}} = \mathbf{AX} + \mathbf{BU}$$

The bold letters indicate that **X**, **A**, **B**, **U** are matrices. **X** is the state vector matrix, the elements comprising the state variables; **A** is the state coefficient matrix; **B** is the driving matrix; **U** is the control input vector matrix, the elements comprising the control input variables.

For example, in Eq. (3.43), the state variables v, p, r, Φ form the state vector

$$\mathbf{X} = \begin{bmatrix} v \\ p \\ r \\ \Phi \end{bmatrix}$$

The state coefficient matrix

$$\mathbf{A} = \begin{bmatrix} \frac{Y_v}{m} & W_0 & -U_0 & g \\ \frac{L_v}{I_x} & \frac{L_p}{I_x} & \frac{L_r}{I_x} & 0 \\ \frac{N_v}{I_z} & \frac{N_p}{I_z} & \frac{N_r}{I_z} & 0 \\ 0 & 1 & 0 & 0 \end{bmatrix}$$

The driving matrix

$$\mathbf{B} = \begin{bmatrix} \frac{Y_\zeta}{m} & 0 \\ \frac{L_\zeta}{I_x} & \frac{L_\xi}{I_x} \\ \frac{N_\zeta}{I_z} & \frac{N_\xi}{I_z} \\ 0 & 0 \end{bmatrix}$$

The control input vector

$$\mathbf{U} = \begin{bmatrix} \zeta \\ \xi \end{bmatrix}$$

Further treatment of state variable matrix equations is beyond the scope of this chapter, the main objective being to introduce the reader who is not familiar with the methods and terminology to their use. Appropriate textbooks are listed in the 'Further Reading' at the end of this chapter.

3.5 Longitudinal Control and Response

3.5.1 Longitudinal Control

In conventional (i.e. non-fly-by-wire) aircraft, the pilot controls the angular movement of the tailplane/elevators directly from the control column, or 'stick', which is mechanically coupled by rods and linkages to the tailplane/elevator servo actuator. (Fully powered controls are assumed.) To manoeuvre in the longitudinal (or pitch) plane, the pilot controls the tailplane/elevator angle and hence the pitching moment exerted about the CG by the tailplane lift. This enables the pilot to rotate the aircraft about its CG to change

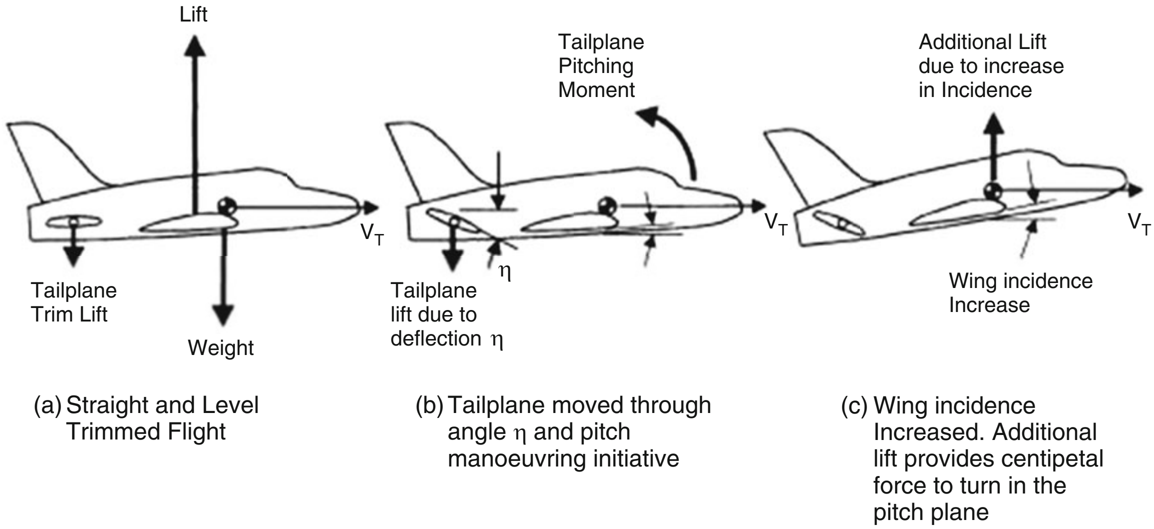

Fig. 3.24 Manoeuvring in the pitch plane

the wing incidence angle and hence control the wing lift to provide the necessary normal, or centripetal, force to change the direction of the aircraft's flight path (see Fig. 3.24).

The initial response of the aircraft on application of a steady tailplane/elevator angular movement from the trim position is as follows.

The resulting pitching moment accelerates the aircraft's inertia about the pitch axis causing the aircraft to rotate about its CG so that the wing incidence angle increases. The wing lift increases accordingly and causes the aircraft to turn in the pitch plane and the rate of pitch to build up. This rotation about the CG is opposed by the pitching moment due to incidence which increases as the incidence increases and by the pitch rate damping moment exerted by the tailplane. A steady condition is reached and the aircraft settles down to a new steady wing incidence angle and a steady rate of pitch which is proportional to the tailplane/elevator angular movement from the trim position.

The aircraft's inertia about the pitch axis generally results in some transient overshoot before a steady wing incidence is achieved, the amount of overshoot being mainly dependent on the pitch rate damping generated by the tailplane.

The normal acceleration is equal to the product of the forward speed and the rate of pitch and is directly proportional to the increase in wing lift resulting from the increase in wing incidence angle. For a given constant forward speed, the rate of pitch is thus proportional to the tailplane/elevator angular movement from the trim position, which in turn is proportional to the stick deflection. The rate of pitch is reduced to zero by returning, that is 'centralising', the stick to its trimmed flight position.

3.5.2 Stick Force/g

The wing lift is, however, proportional to both the wing incidence and the dynamic pressure, $\frac{1}{2}\rho V_T^2$, so the required wing incidence for a given normal acceleration will vary with height and speed over the flight envelope. Only a small change in wing incidence is required at the high dynamic pressures resulting from high-speed low-level flight, and vice versa.

The tailplane/elevator angular movement required per *g* normal acceleration, and hence stick displacement/*g*, will thus vary with height and speed: the variation can be as high as 40:1 over the flight envelope for a high-performance aircraft.

The aerodynamic forces and moments are proportional to the dynamic pressure and with manually operated flying controls (i.e. no hydraulically powered controls), the pilot has a direct feedback from the stick of the forces being exerted as a result of moving the elevator. Thus, at higher speeds and dynamic pressures only a relatively small elevator movement is required per *g* normal acceleration. The high dynamic pressure experienced, however, requires a relatively high stick force although the stick movement is small. At lower speeds and dynamic pressures, a larger elevator angle is required per *g* and so the stick force is still relatively high. The stick force/*g* thus tends to remain constant for a well-designed aeroplane operating over its normal flight envelope.

However, with the fully powered flying controls required for high-speed aircraft, there is no direct feedback at the stick of the control moments being applied by moving the tailplane/elevators.

Stick displacement is an insensitive control for the pilot to apply, stick force being a much more natural and effective control, and matches with the pilot's experience and training flying aircraft with manually operated controls.

The stick force is made proportional to stick deflection by either a simple spring loading system or by an '*artificial feel unit*' connected directly to the stick mechanism. The artificial feel unit varies the stick stiffness (or 'feel') as a function of dynamic pressure $\frac{1}{2}\rho V_T^2$ so as to provide the required stick force/g characteristics. The rate of pitch at a given forward speed (i.e. normal acceleration) is thus made proportional to the stick force applied by the pilot. However, as already mentioned, the effectiveness of the tailplane/elevator can vary over a wide range over the height and speed envelope. Automatic control may be required to improve the aircraft response and damping over the flight envelope and give acceptable stick force per g characteristics.

3.5.3 Pitch Rate Response to Tailplane/Elevator Angle

The key to analysing the response of the aircraft and the modifying control required from the automatic flight control system is to determine the aircraft's basic control transfer function. This relates the aircraft's pitch rate, q, to the tailplane/elevator angular movement, η, from the trimmed position.

This can be derived from Eqs. (3.34), (3.35) and (3.36) together with the relationship $q = d\theta/dt$ by eliminating u and w to obtain an equation in q and η only. This results in a transfer function of the form below:

$$\frac{q}{\eta} = \frac{K\left(D^3 + b_2 D^2 + b_1 D + b_0\right)}{\left(D^4 + a_3 D^3 + a_2 D^2 + a_1 D + a_0\right)}$$

where $D = d/dt$.

K, b_2, b_1, b_0, a_3, a_2, a_1, a_0 are constant coefficients comprising the various derivatives. The transient response (and hence the stability) is determined by the solution of the differential equation $(D^4 + a_3 D^3 + a_2 D^2 + a_1 D + a_0)q = 0$.

$q = Ce^{\lambda t}$, where C and λ are constants, is a solution of this type of linear differential equation with constant coefficients. Substituting $Ce^{\lambda t}$ for q yields

$$\left(\lambda^4 + a_3\lambda^3 + a_2\lambda^2 + a_1\lambda + a_0\right)Ce^{\lambda t} = 0$$

That is,

$$\left(\lambda^4 + a_3\lambda^3 + a_2\lambda^2 + a_1\lambda + a_0\right) = 0$$

This equation is referred to as the characteristic equation. This quartic equation can be split into two quadratic factors, which can be further factorised into pairs of conjugate complex factors as shown below:

$$(\lambda + \alpha_1 + j\omega_1)(\lambda + \alpha_1 - j\omega_1)(\lambda + \alpha_2 + j\omega_2) \times (\lambda + \alpha_2 - j\omega_2) = 0$$

The solution is as follows:

$$q = \underbrace{A_1 e^{-\alpha_1 t}\sin(\omega_1 t + \phi_1)}_{\text{Short period motion}} + \underbrace{A_2 e^{-\alpha_2 t}\sin(\omega_2 t + \phi_2)}_{\text{Long period motion}}$$

A_1, ϕ_1, A_2, ϕ_2 are constants determined by the initial conditions, that is, value of $\ldots q$, $\ddot{q}$, $\dot{q}$, q at time $t = 0$.

For the system to be stable, the exponents must be negative so that the exponential terms decay to zero with time. (Positive exponents result in terms which diverge exponentially with time, i.e. an unstable response.)

The solution thus comprises the sum of two exponentially damped sinusoids corresponding to the short-period and long-period responses, respectively.

The initial basic response of the aircraft is thus a damped oscillatory response known as the short-period response. The period of this motion is in the region of 1 to 10 seconds, depending on the type of aircraft and its forward speed, being inversely proportional to the forward speed, for example, typical fighter aircraft would be about 1-second period whereas a large transport aircraft would be about 5- to 10-second period. This short-period response is generally fairly well-damped for a well-behaved (stable) aircraft but may need augmenting with an auto-stabilisation system over parts of the flight envelope of height and speed combinations.

The second stage comprises a slow lightly damped oscillation with a period ranging from 40 seconds to minutes and is known as the long period/motion. It is basically similar to the *phugoid* motion and is again inversely proportional to forward speed. The phugoid motion consists of a lightly damped oscillation in height and airspeed whilst the angle of incidence remains virtually unchanged and is due to the interchange of kinetic energy and potential energy as the aircraft's height and speed change. The damping of the phugoid motion is basically a task for the autopilot, the long period making it very difficult for the pilot to control.

Figure 3.25 illustrates the two types of motion in the response.

A simpler method of obtaining a good approximation to the *q/n* transfer function, which accurately represents the aircraft's short-period response, can be obtained by assuming the forward speed remains constant. This is a reasonable assumption as the change in forward speed is slow compared with the other variables.

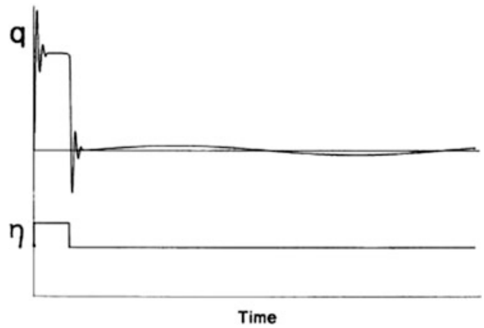

Fig. 3.25 Pitch response

This simpler method is set out in the next section as it gives a good 'picture' in control engineering terms of the behaviour of the basic aircraft.

3.5.4 Pitch Response Assuming Constant Forward Speed

The transfer functions relating pitch rate and wing incidence to tailplane (or elevator) angle, that is q/η and α/η, are derived below from first principles making the assumption of constant forward speed and small perturbations from steady straight and level, trimmed flight.

The derivative terms due to the rate of change of vertical velocity, $\dot{w}$, that is $Z_{\dot{w}}\dot{w}$ and $M_{\dot{w}}\dot{w}$, are neglected and also the $Z_{\mathrm{q}}q$ term.

Referring to Fig. 3.26, an orthogonal set of axes OX, OY, OZ moving with the aircraft with the centre O at the aircraft's centre of gravity is used to define the aircraft motion. OX is aligned with the flight path vector, OY with the aircraft's pitch axis and OZ normal to the aircraft's flight path vector (positive direction downwards). These axes are often referred to as 'stability axes' and enable some simplification to be achieved in the equations of motion.

Velocity along OX axis is U (constant); velocity increment along OZ axis is w; velocity along OY axis is 0; rate of rotation about pitch axis, OY, is q; change in angle of incidence from trim value is α; aircraft mass is m; aircraft moment of inertia about pitch axis, OY, is I_{y}.

Considering forces acting in OZ direction:

1. Change in lift force acting on wing due to change in angle of incidence, α, from trim value is $Z_{\alpha}\alpha$.
2. Change in lift force acting on tailplane due to change in tailplane angle, η, from trim value is $Z_{\eta}\eta$.

Normal acceleration along OZ axis is $\dot{w} - Uq$, where $\dot{w} = dw/dt$ (refer to Sect. 3.4.3, Eq. (3.21)).

Equation of motion along OZ axis is

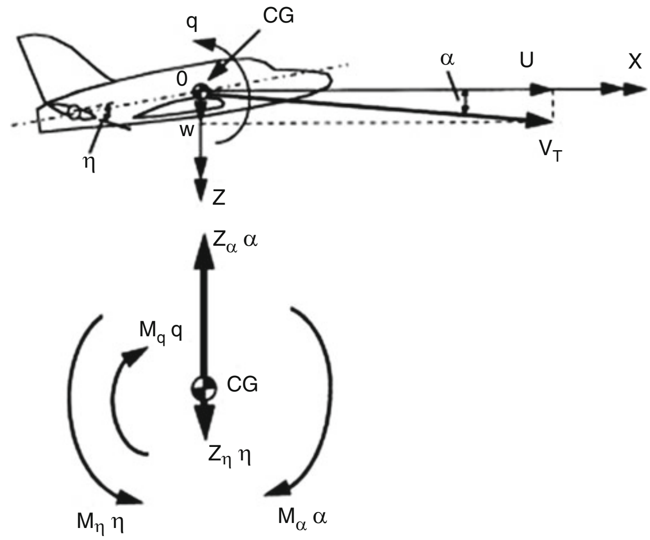

Fig. 3.26 Forces and moments – longitudinal plane (stability axes)

$$Z_{\alpha}\alpha + Z_{\eta}\eta = m\left(\dot{w} - U_{\mathrm{q}}\right) \tag{3.44}$$

Considering moments acting about CG:

1. Pitching moment due to change in tailplane angle, η, from trim value is $M_{\eta}\eta$.
2. Pitching moment due to change in angle of incidence, α, from trim value is $M_{\alpha}\alpha$.
3. Pitching moment due to angular rate of rotation, q, about the pitch axis is $M_{\mathrm{q}}q$.

Equation of angular motion about pitch axis, OY, is

$$M_{\eta}\eta + M_{\alpha}\alpha + M_{\mathrm{q}}q = I_{\mathrm{y}}\dot{q} \tag{3.45}$$

where $\dot{q} = dq/dt$ is angular acceleration and change in angle of incidence is

$$\alpha = \frac{w}{U} \tag{3.46}$$

These simultaneous differential equations can be combined to give equations in terms of q and η only by eliminating w, or, α and η only by eliminating q. However, it is considered more instructive to carry out this process using block diagram algebra as this gives a better physical picture of the aircraft's dynamic behaviour and the inherent feedback mechanisms relating q and α.

Equation (3.45) can be written as

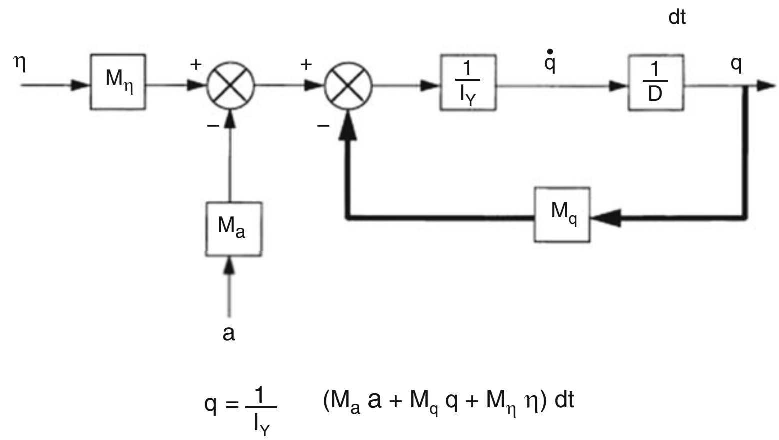

Fig. 3.27 Block diagram representation of Eq. (3.47)

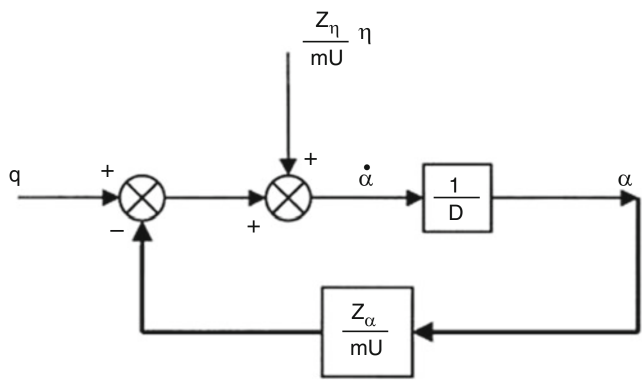

Fig. 3.28 Block diagram representation of Eq. (3.48)

$$q = \frac{1}{I_{\mathrm{y}}}\int \left(M_{\alpha}\alpha + M_{\mathrm{q}}q + M_{\eta}\eta\right)dt \tag{3.47}$$

Substituting $U\dot{\alpha}$ for w in Eq. (3.44) and re-arranging yields

$$\alpha = \int \left(q + \frac{Z_{\alpha}}{mU}\alpha + \frac{Z_{\eta}}{mU}\eta\right)dt \tag{3.48}$$

Figure 3.27 represents Eq. (3.47) in block diagram form. It should be noted that the signs of the derivatives have been indicated at the summation points in the block diagram. M_{q} is negative and an aerodynamically stable aircraft is assumed so that M_{α} is also negative. The $M_{\mathrm{q}}q$ and $M_{\alpha}\alpha$ terms are thus negative feedback terms. (Positive M_{α} can be allowed for by the appropriate sign change.) Figure 3.28 is a block diagram representation of Eq. (3.48).

The q and α subsidiary feedback loops can be simplified using the relationship between output, θ_{o}, and input, θ_{i}, in a generalised negative feedback process of the type shown in Fig. 3.29.

That is,

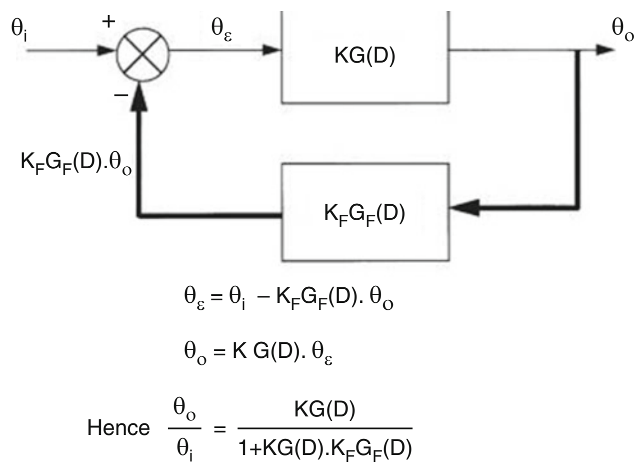

Fig. 3.29 Generalised negative feedback system

$$\frac{\theta_{\mathrm{o}}}{\theta_{\mathrm{i}}} = \frac{KG(D)}{1 + KG(D)\cdot K_{\mathrm{F}}G_{\mathrm{F}}(D)} \tag{3.49}$$

where $KG(D)$ and $K_{\mathrm{F}}G_{\mathrm{F}}(D)$ are the transfer functions of the forward path and feedback path, respectively.

Thus, considering the $M_{\mathrm{q}}q$ feedback loop

$$\frac{q}{(M_{\eta}\eta - M_{\alpha}\alpha)} = \frac{\frac{1}{I_{\mathrm{y}}D}}{1 + \frac{1}{I_{\mathrm{y}}D}\cdot M_{\mathrm{q}}}$$

as $KG(D) = 1/I_{\mathrm{y}}D$ and $K_{\mathrm{F}}G_{\mathrm{F}}(D) = M_{\mathrm{q}}$.

$$\frac{q}{(M_{\eta}\eta - M_{\alpha}\alpha)} = \frac{1}{M_{\mathrm{q}}}\cdot\frac{1}{(1 + T_1 D)} \tag{3.50}$$

where

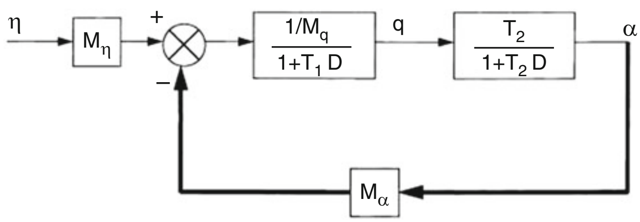

Fig. 3.30 Simplified overall block diagram

$$T_1 = \frac{I_y}{M_q} \tag{3.51}$$

This represents a simple first-order lag transfer function.

Referring to Fig. 3.28, the *α/q* inner loop can be similarly simplified to

$$\frac{\alpha}{q} = T_2 \cdot \frac{1}{(1 + T_2 D)} \tag{3.52}$$

where

$$T_2 = \frac{mU}{Z_\alpha} \tag{3.53}$$

This represents another first-order lag transfer function. The overall block diagram thus simplifies to Fig. 3.30.

It should be noted that the $Z_\eta \eta / mU$ input term has been omitted for simplicity as it is small in comparison with the other terms. Also, because it is an external input to the loop, it does not affect the feedback loop stability and transient response to a disturbance.

Referring to Fig. 3.30 and applying Eq. (3.49) yields

$$\frac{q}{\eta} = M_\eta \cdot \frac{\frac{\frac{1}{M_q}}{(1+T_1 D)}}{1 + \frac{\frac{1}{M_q}}{(1+T_1 D)} \cdot \frac{T_2}{(1+T_2 D)} M_\alpha} \tag{3.54}$$

This simplifies to

$$\frac{q}{\eta} = \frac{M_\eta}{I_y T_2} \cdot \frac{(1 + T_2 D)}{D^2 + \left(\frac{1}{T_1} + \frac{1}{T_2}\right) D + \frac{M_\alpha}{I_y} + \frac{1}{T_1 T_2}} \tag{3.55}$$

$$\frac{q}{\eta} = \frac{K(1 + T_2 D)}{\left(D^2 + A_1 D + A^2\right)} \tag{3.56}$$

where

$$K = \frac{M_\eta}{I_y T_2} = \frac{M_\eta Z_\alpha}{I_y m U} \tag{3.57}$$

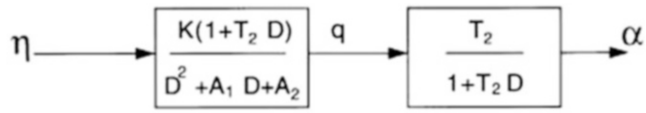

Fig. 3.31 Further simplified overall block diagram

$$A_1 = \frac{1}{T_1} + \frac{1}{T_2} = \frac{M_q}{I_y} + \frac{Z_\alpha}{mU} \tag{3.58}$$

$$A_2 = \frac{M_\alpha}{I_y} + \frac{1}{T_1 T_2} = \frac{M_\alpha}{I_y} + \frac{M_q Z_\alpha}{I_y m U} \tag{3.59}$$

Substituting

$$\alpha = \frac{T_2}{1 + T_2 D} \cdot q$$

in Eq. (3.56) yields

$$\frac{\alpha}{\eta} = \frac{K T_2}{\left(D^2 + A_1 D + A_2\right)} \tag{3.60}$$

The resulting overall block diagram is shown in Fig. 3.31. From Eq. (3.56)

$$\left(D^2 + A_1 D + A_2\right) q = K(1 + T_2 D)\eta \tag{3.61}$$

The transient response is given by the solution of the differential equation

$$\left(D^2 + A_1 D + A_2\right) q = 0 \tag{3.62}$$

The solution is determined by the roots of the characteristic equation

$$\left(\lambda^2 + A_1 \lambda + A_2\right) = 0$$

which are $\lambda = -\frac{1}{2} A_1 \pm \sqrt{A_1{}^2 - 4A_2}/2$.

In a conventional aircraft these are complex roots of the form $-\alpha_1 \pm j\omega$, where $\alpha_1 = A_1/2$ $\omega = \sqrt{4A_2 - A_1{}^2}/2$.

The solution in this case is an exponentially damped sinusoid

$$q = A e^{-\alpha_1 t} \sin(\omega t + \phi)$$

when A and ϕ are constants determined from the initial conditions (value of $\dot{q}$ and q at time $t = 0$). The coefficient A_1 determines the value of α_1 ($= A_1/2$) and this determines the degree of damping and overshoot in the transient

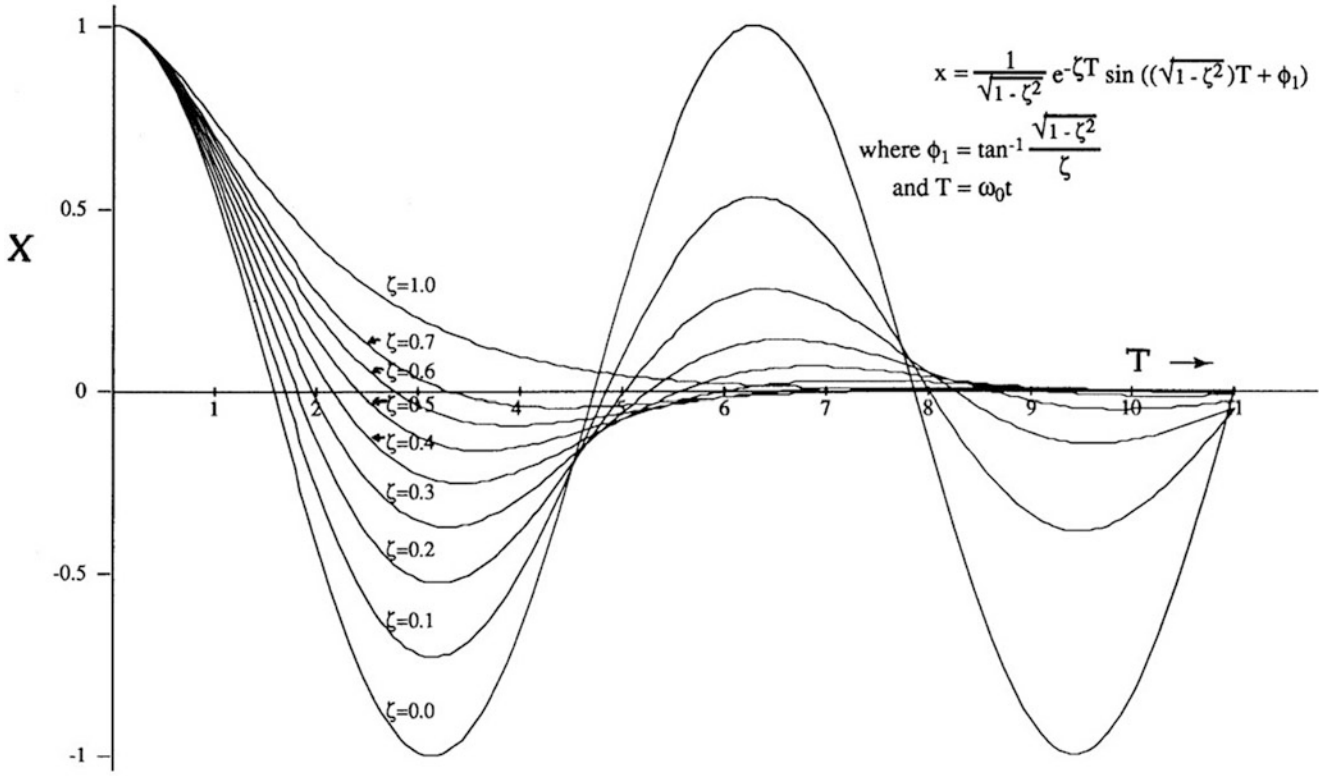

Fig. 3.32 Generalised second-order system transient response

response to a disturbance. The coefficient A_2 largely determines the frequency, ω, of the damped oscillation $\omega = \sqrt{4A_2 - {A_1}^2}/2$ and hence the speed of the response.

In order for the system to be stable the roots of the characteristic equation must be negative or have a negative real part, so that the exponents are negative and exponential terms decay to zero with time. This condition is met provided A_1 and A_2 are both positive.

Conversely, an aerodynamically unstable aircraft with a positive M_α would result in A_2 being negative thereby giving a positive exponent and a solution which diverges exponentially with time.

It is useful to express the quadratic factor $(D^2 + A_1 D + A_2)$ in terms of two generalised parameters ω_0 and ζ, thus $(D^2 + 2\zeta\omega_0 D + \omega_0^2)$ where ω_0 is the undamped natural frequency $= \sqrt{A_2}$.

$$\zeta = \text{Damping ratio} = \frac{\text{Coefficient of } D}{\text{Coefficient of } D \text{ for critical damping}}$$

That is,

$$\zeta = \frac{A_1}{2\sqrt{A_2}} \tag{3.63}$$

(Critical damping results in a non-oscillatory response and is the condition for equal roots, which occurs when $A_1^2 = 4A_2$.)

The transient response to an initial disturbance to a general second-order system of the type $(D^2 + 2\zeta\omega_0 D + \omega_0^2)x = 0$ when x is any variable is plotted out in Fig. 3.32 for a range of values of damping ratio, ζ, and non-dimensional time $T = \omega_0 t$. These graphs can be used for any second-order system.

The steady-state values on application of a given tailplane (or elevator) angle can be obtained for both pitch rate and incidence by equating all the terms involving rates of change to zero. Thus in Eq. (3.61), $\ddot{q}$, $\dot{q}$ and $\dot{\eta}$ are all zero in the steady state. The suffix ss is used to denote steady-state values.

Whence $A_2 q_{ss} = K\eta_{ss}$

$$q_{ss} = \frac{K}{A_2}\eta_{ss} \tag{3.64}$$

The steady-state change in wing incidence, α_{ss}, can be obtained in a similar manner from Eq. (3.60) and is given by

$$\alpha_{ss} = \frac{KT_2}{A_2}\eta_{ss} \tag{3.65}$$

It can be seen that changes in the aerodynamic derivatives over the flight envelope will alter both the speed and damping of the transient response to a tailplane movement or a disturbance. The steady-state wing incidence and pitch rate for a given tailplane (or elevator) movement will also change and hence the *Stick Force per g* will change over the flight envelope.

3.5.5 Worked Example on q/η Transfer Function and Pitch Response

The aerodynamic data below are very broadly representative of a conventional combat aircraft of transonic performance. These data have been derived by a 'reverse engineering' process from a knowledge of typical control 'gearings' in flight control systems (e.g. control surface movement/g) and actual aircraft short-period responses in terms of undamped natural frequency and damping ratio.

The objective of the worked example is to try to bring together the basic aerodynamic and aircraft control theory presented so far and show how this can be applied to give an appreciation of the aircraft's pitch response and also the need for auto-stabilisation.

The data and calculations are rounded off to match the accuracy of the estimates, and the aerodynamic behaviour has been greatly simplified and compressibility effects, etc., ignored.

In practice, the necessary aerodynamic derivative data would normally be available. The worked example below has been structured to bring out some of the aerodynamic relationships and principles.

Aircraft Data

Aircraft mass, $m = 25{,}000$ kg (55,000 lb)
Forward speed, $U = 250$ m/s (500 knots approx.)
Moment of inertia about pitch axis, $I_y = 6 \times 10^5$ kg m^2
Pitching moment due to incidence, $M_\alpha = 2 \times 10^7$ Nm/radian
Tailplane moment arm, $l_t = 8$ m
Wing incidence/g: 1.6° increase in wing incidence at 500 knots produces 1 g normal acceleration
Tailplane angle/g: 1° tailplane angular movement produces 1 g normal acceleration at 500 knots

Questions

(a) Derive an approximate *q/n* transfer function, assuming forward speed is constant.
(b) What is the undamped natural frequency and damping ratio of the aircraft's pitch response?
(c) What is the percentage overshoot of the transient response to a disturbance or control input?

$$\frac{q}{\eta} = \frac{K(1 + T_2 D)}{D^2 + A_1 D + A_2}$$

The problem is to derive K, T_2, A_1 and A_2 from the data given.

The undamped natural frequency, $\omega_0 = \sqrt{A_2}$, and damping ratio $\zeta = A_1/2\sqrt{A_2}$ can then be calculated knowing A_1 and A_2.

- *Derivation of* T_2
  Increase in wing lift is $Z_\alpha \alpha = m(ng)$
  where (ng) is normal acceleration
  1.6° change in wing incidence produces 1g normal acceleration at 500 knots
  Hence $Z_\alpha\ 1.6/60 = m\ 10$
  (Taking $1° \approx 1/60$ radian and $g \approx 10$ m/s^2)
  That is, $Z_\alpha = 375$ m
  $T_2 = mU/Z_\alpha = m\ 250/375$ m
  That is, $T_2 = 0.67$ s.
- *Relationship between* M_q *and* M_η
  Assuming an all moving tailplane
  Pitching moment due to tailplane angle change, $\eta = M_\eta \eta$
  Change in tailplane incidence due to pitch rate, $q = l_t\, q/U$
  Pitching moment due to pitch rate is $M_\eta l_t q/U = M_q q$
  Hence for an all moving tailplane, $M_q = l_t/U \cdot M_\eta$
  $l_t = 8$ m, $U = 250$ m/s
  $M_q = 8/250 \cdot M_\eta = 0.032 M_\eta$.
- *Derivation of* M_η *and* M_q
  1 g normal acceleration at 250 m/s forward speed corresponds to a rate of pitch equal to 10/250 rad/s, that is 2.4°/s approx. (taking $g = 10$ m/s^2).
  1.6° change in wing incidence produces 1g normal acceleration and requires 1° tailplane angular movement.
  Thus in the steady state (denoted by suffix *ss*), $M_\eta \eta_{ss} = M_\alpha \alpha_{ss} + M_q q_{ss}$
  Working in degrees, $M_\eta \cdot 1 = (2 \times 10^7 \times 1.6) + (0.032 M_\eta \times 2.4)$
  Hence, $M_\eta = 3.5 \times 10^7$ Nm/rad and $M_q = 0.032 \times 3.5 \times 10^7$ Nm/rad/s, that is, $M_q = 1.1 \times 10^6$ Nm/rad/s.

- *Derivation of T_1*

$$T_1 = \frac{6 \times 10^5}{1.1 \times 10^6}$$

That is, $T_1 = 0.55$ s.

- *Derivation of coefficient A_1*

$$A_1 = \frac{1}{T_1} + \frac{1}{T_2} + \frac{1}{0.55} + \frac{1}{0.67}$$

That is, $A_1 = 2.3$.

- *Derivation of coefficient A_2*

$$A_2 = \frac{M_\alpha}{I_y} + \frac{1}{T_1 T_2} = \frac{2 \times 10^7}{6 \times 10^5} + \frac{1}{0.55 \times 0.67}$$

That is, $A_2 = 36$.

- *Derivation of K*

$$K = \frac{M_\eta}{I_y T_2} = \frac{3.5 \times 10^7}{6 \times 10^5 \times 0.67}$$

That is, $K = 87$.
Hence

$$\frac{q}{\eta} = \frac{87(1 + 0.67D)}{\left(D^2 + 2.3D + 36\right)}$$

By inspection $\omega_0^2 = 36$

- That is, $\omega_0 = 6$ rad/s (0.95 Hz)

$$\zeta = 2.3/(2 \times 6)$$

- That is, $\zeta = 0.2$ approx.

From examination of second-order system responses in Fig. 3.32.

Percentage overshoot of response to a disturbance or control input is just over 50%.

- *A candidate for auto-stabilisation*

These data will be used in a worked example on auto-stabilisation in Sect. 3.8.

3.6 Lateral Control

3.6.1 Aileron Control and Bank to Turn

The primary means of control of the aircraft in the lateral plane are the ailerons (see Fig. 3.15). These are moved differentially to increase the lift on one wing and reduce it on the other thereby creating a rolling moment so that the aircraft can be banked to turn.

Aircraft bank to turn so that a component of the wing lift can provide the essential centripetal force towards the centre of the turn in order to change the aircraft's flight path (see Fig. 3.33). The resulting centripetal acceleration is equal to (aircraft velocity) × (rate of turn), that is, $V_T\dot{\Psi}$. This centripetal acceleration causes an inertia force to be experienced in the reverse direction, that is, a centrifugal force.

In a steady banked turn with no sideslip the resultant force the pilot experiences is the vector sum of the gravitational force and the centrifugal force and is in the direction normal to the wings. The pilot thus experiences no lateral forces.

Banking to turn is thus fundamental to effective control and manoeuvring in the lateral plane because of the large lift forces that can be generated by the wings. The lift force can be up to nine times the aircraft weight in the case of a modern fighter aircraft. The resulting large centripetal component thus enables small radius, high g turns to be executed.

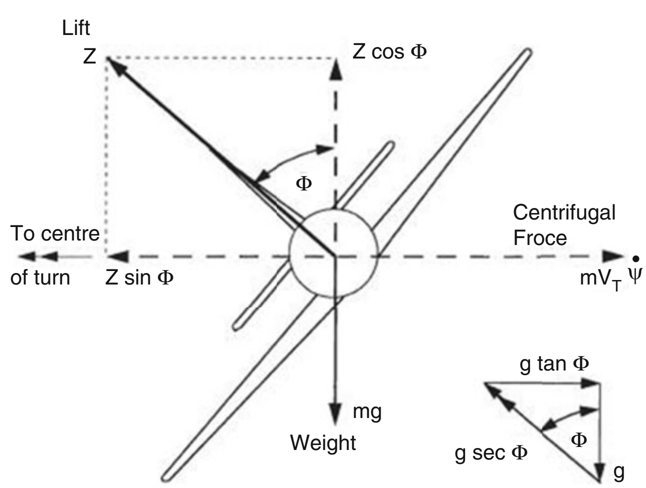

Fig. 3.33 Forces acting in a turn

Referring to Fig. 3.33: Horizontal component of the lift force is $Z \sin \Phi$. Equating this to the centrifugal acceleration gives

$$Z \sin \Phi = mV_T\dot{\Psi}$$

Vertical component of the lift force is $Z \cos \Phi$. Equating this to the aircraft weight gives

$$Z \cos \Phi = mg$$

from which

$$\tan \Phi = \frac{V_T\dot{\Psi}}{g} \tag{3.66}$$

Thus the acceleration towards the centre of the turn is $g \tan \Phi$.

Referring to the inset vector diagram in Fig. 3.33, the normal acceleration component is thus equal to $g \sec \Phi$. Thus, a 60° banked turn produces a centripetal acceleration of 1.73 g and a normal acceleration of 2 g. At a forward speed of 100 m/s (200 knots approx.) the corresponding rate of turn would be 10.4°/s.

The lift required from the wings increases with the normal acceleration and the accompanying increase in drag requires additional engine thrust if the forward speed is to be maintained in the turn. The ability to execute a high g turn thus requires a high engine thrust/aircraft weight ratio.

To execute a coordinated turn with no sideslip requires the operation of all three sets of control surfaces, that is the ailerons and the tailplane (or elevator) and to a lesser extent the rudder. It is also necessary to operate the engine throttle (s) to control the engine thrust. The pilot first pushes the stick sideways to move the ailerons so that the aircraft rolls, the rate of roll being dependent on the stick movement. The rate of roll is arrested by centralising the stick when the desired bank angle for the rate of turn has been achieved. The pilot also pulls back gently on the stick to pitch the aircraft up to increase the wing incidence and hence the wing lift to stop loss of height and provide the necessary centripetal force to turn the aircraft. A gentle pressure is also applied to the rudder pedals as needed to counteract the yawing moment created by the differential drag of the ailerons. The throttles are also moved as necessary to increase the engine thrust to counteract the increase in drag resulting from the increase in lift and hence maintain airspeed.

The dynamics of the aircraft response to roll commands are complex and are covered later in Sect. 3.6.4. However, an initial appreciation can be gained by making the simplifying assumption of pure rolling motion, as follows.

Angular movement of the ailerons from the trim position, ξ, produces a rolling moment equal to $L_\xi\xi$ where L_ξ is the rolling moment derivative due to aileron angle movement. This is opposed by a rolling moment due to the rate of roll (refer to Sect. 3.4.4.2 and Fig. 3.23), which is equal to L_pp. The equation of motion is thus

$$L_\xi\xi + L_p p = I_x\dot{p} \tag{3.67}$$

where I_x is moment of inertia of the aircraft about the roll axis.

This can be expressed in the form

$$(1 + T_R D)p = \frac{L_\xi}{L_p} \cdot \xi \tag{3.68}$$

where T_R is the roll response time constant $= I_x / - L_p$ (note L_p is negative).

This is a classic first-order system, the transient solution being $p = Ae^{-t/TR}$, where A is a constant determined by the initial conditions.

For a step input of aileron angle, ξ_i, the response is given by

$$p = \frac{L_\xi}{L_p}\left(1 - e^{-1/T_R}\right)\xi \tag{3.69}$$

This is illustrated in Fig. 3.34.

It can be seen that variations in the derivatives L_p and L_ξ over the flight envelope will affect both the speed of response and the steady-state rate of roll for a given aileron movement. It should be noted that aerodynamicists also refer to the roll response as a subsidence as this describes the exponential decay following a roll rate disturbance.

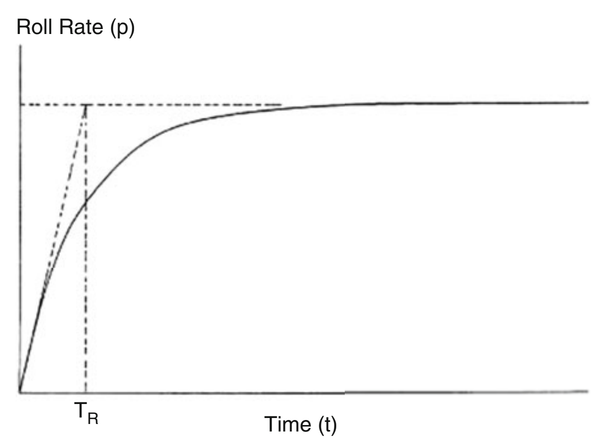

Fig. 3.34 Roll rate response

3.6.2 Rudder Control

Movement of the rudder creates both a lateral force and a yawing moment. The control action exerted by the rudder is thus used to:

(a) Counteract the yawing moment due to movement of the ailerons to bank the aircraft to turn as already explained.
(b) Counteract sideslipping motion.
(c) Counteract asymmetrical yawing moments resulting, say, from loss of engine power in the case of multi-engine aircraft or carrying asymmetrical stores/weapons in the case of a combat aircraft (or both).
(d) Deliberate execution of a sideslipping manoeuvre. The yawing moment created by the rudder movement will produce a sideslip incidence angle, β, and this will result in a side force from the fuselage and fin (see Fig. 3.21). This side force enables a flat sideslipping turn to be made. However, the sideways accelerations experienced in flat turns are not comfortable for the pilot (or crew and passengers for that matter). In any case, the amount of sideways lift that can be generated by the fin and fuselage body will only enable very wide flat turns to be made in general.
(e) To ‘kick-off’ the drift angle just prior to touch down when carrying out a crosswind landing. This is to arrest any sideways motion relative to the runway and so avoid side forces acting on the undercarriage at touch down.

Directional stability in the lateral plane is provided by the fin and rudder. Referring to Fig. 3.21, a sideslip velocity, v, with the aircraft’s fore and aft axis at an incidence angle, β, to the aircraft velocity vector, V_T, (or relative wind) results in the fin developing a side force. As explained earlier, this side force tends to align the aircraft with the relative wind in a similar manner to a weathercock.

3.6.3 Short-Period Yawing Motion

This weathercock action can result in a lightly damped oscillatory motion under certain flight conditions because of the aircraft’s inertia, if the yaw rate damping moment is small. The analysis of this motion can be simplified by assuming pure yawing motion and neglecting the cross-coupling of yawing motion with rolling motion (and vice versa). The direction of the aircraft’s velocity vector is also assumed to be unchanged.

(It should be noted that the lateral response allowing for the effects of the roll/yaw cross-coupling is covered later in Sect. 3.6.4.) Referring to Fig. 3.21, it can be seen that:

$$\text{Sideslip velocity, } v = V_T \sin\beta = V_T\beta (\text{as } \beta \text{ is a small angle}) = V_T\psi$$

as $\beta = \psi$, the incremental change in heading (or yaw) angle.

Thus yawing moment due to sideslip is $N_v V_T \psi$.

It should be noted that in general the yaw angle ψ is not the same as the sideslip incidence angle β, the yaw angle being the angle in the lateral plane between the aircraft’s fore and aft axis and the original direction of motion. The two angles are only the same when the direction of the aircraft’s velocity vector is unchanged. The moments acting about the CG are as follows:

1. Yawing moment due to sideslip is $N_v V_T \psi$.
2. Yawing moment due to yaw rate is $N_r r = N_r \dot{\Psi}$.

The equation of motion is as follows:

$$N_v V_T \Psi + N_r \dot{\Psi} = I_z \ddot{\Psi} \tag{3.70}$$

where I_z is moment of inertia about yaw axis.

That is,

$$\left(D^2 + \frac{-N_r}{I_z} D + \frac{-N}{I_z} V_T\right)\Psi = 0 \tag{3.71}$$

Note that derivatives N_r and N_v are both negative.

This is a second-order system with an undamped natural frequency

$$\omega_0 = \sqrt{\frac{N_v V_T}{I_z}}$$

and damping ratio

$$\zeta = \frac{1}{2}\frac{N_r}{\sqrt{N_v V_T I_z}}$$

Both the period of the oscillation $(2\pi/\omega_0)$ and the damping ratio are inversely proportional to the square root of the forward speed, that is, $\sqrt{V_T}$. Thus increasing the speed shortens the period but also reduces the damping. The period of the oscillation is of the order of 3 to 10 seconds.

This short-period yawing motion can be effectively damped out automatically by a yaw axis stability augmentation system (SAS) (or yaw damper) and will be covered in Sect. 3.7.

In practice there can be a significant cross-coupling between yawing and rolling motion and the yawing oscillatory motion can induce a corresponding oscillatory motion about the roll axis 90° out of phase known as '*Dutch roll*'. (Reputedly after the rolling–yawing gait of a drunken Dutchman.) The ratio of the amplitude of the rolling motion to that of the yawing motion is known as the '*Dutch roll ratio*' and can exceed unity, particularly with aircraft with large wing sweepback angles.

3.6.4 Combined Roll–Yaw–Sideslip Motion

The cross-coupling and interactions between rolling, yawing and sideslip motion and the resulting moments and forces have already been described in Sect. 3.4.4.2. The interactions between rudder and aileron controls have also been mentioned.

The equations of motion in the lateral plane following small disturbances from straight and level flight are set out in Sect. 3.4.5, Eqs. (3.37), (3.38) and (3.39), respectively.

The solution to this simplified lateral set of equations in terms of the transient response to a disturbance and resulting stability is a fifth-order differential equation. This can usually be factorised into two complex roots and three real roots as shown below.

$$\left(D^2 + 2\zeta\omega_0 D + \omega_0^2\right)\left(D + \frac{1}{T_{\mathrm{R}}}\right)\left(D + \frac{1}{T_Y}\right)\left(D + \frac{1}{T_{\mathrm{Sp}}}\right)x = 0$$

where x denotes any of the variables v, p, r.

The transient solution is of the form

$$x = A_1 e^{-\zeta\omega_0 t}\sin\left(\sqrt{1-\zeta^2}\cdot\omega_0 t + \phi\right) + A_2 e^{-t/T_{\mathrm{R}}} + A_3 e^{-t/T_{\mathrm{Y}}} + A_4 e^{-t/T_{\mathrm{Sp}}}$$

where A_1, ϕ, A_2, A_3 and A_4 are constants determined by the initial conditions.

The quadratic term describes the Dutch roll motion with undamped natural frequency ω_0 and damping ratio ζ. T_{R} describes the roll motion subsidence and T_{Y} the yaw motion subsidence.

T_{Sp} is usually negative and is the time constant of a slow spiral divergence. It is a measure of the speed with which the aircraft, if perturbed, would roll and yaw into a spiral dive because of the rolling moment created by the rate of yaw. The time constant of this spiral divergence is of the order of 0.5–-1 minute and is easily corrected by the pilot (or autopilot).

3.7 Powered Flying Controls

3.7.1 Introduction

It is appropriate at this point to introduce the subject of mechanically signalled powered flying controls as this is relevant to Sect. 3.8 'Stability Augmentation Systems' and also to Chap. 4.

The forces needed to move the control surfaces of a jet aircraft become very large at high speeds and are too high to be exerted manually. The control surfaces are thus fully power operated with no mechanical reversion; the actuators must also be irreversible to avoid flutter problems.

The hydraulic servo actuation systems which move the main control surfaces are known as *Power Control Units* (PCUs). The PCU is also an essential part of an FBW control system; there are, however, a number of modifications required to adapt the PCU for use in an FBW system as will be explained in the next chapter.

Figure 3.35 shows the mechanically signalled flying control system of the BAE Systems Hawk aircraft to give an appreciation of a typical system.

Figure 3.36 is a schematic illustration of the operation of a PCU. Movement of the control column (or rudder bar) is transmitted through mechanical rods and linkages to the PCU servo control valve. The resulting displacement of the control valve allows high-pressure hydraulic fluid to act on one side of the actuator ram whilst the other side of the ram is connected to the exhaust (or tank) pressure of the hydraulic supply.

The ram moves and this movement is fed back through a mechanical linkage so as to close the valve. The actuator ram thus follows the control column movement with little lag – a simple follow-up type of servo mechanism. A more detailed explanation together with the derivation of the PCU transfer function is given in the next subsection.

Typical hydraulic pressure for a PCU is 200 bar or 20 MPa (3000 psi), so that the actuator can exert a force of several tonnes, depending on the ram cross-sectional area. The forces required to move the PCU valve are small – of the order of a kilogram or less. The pilot, however, can exert a force of 50 kg on the servo control valve, if necessary, to overcome a jammed valve. Although this is a very unlikely event, the airworthiness authorities cite the case of a piece of locking wire getting past the oil filter and jamming the control valve. A force of 50 kg is deemed sufficient to shear through any such obstruction; hence, the relatively hefty yokes, or control columns, and the mechanical advantage built into the linkage/control rod system to enable the pilot to exert such forces.

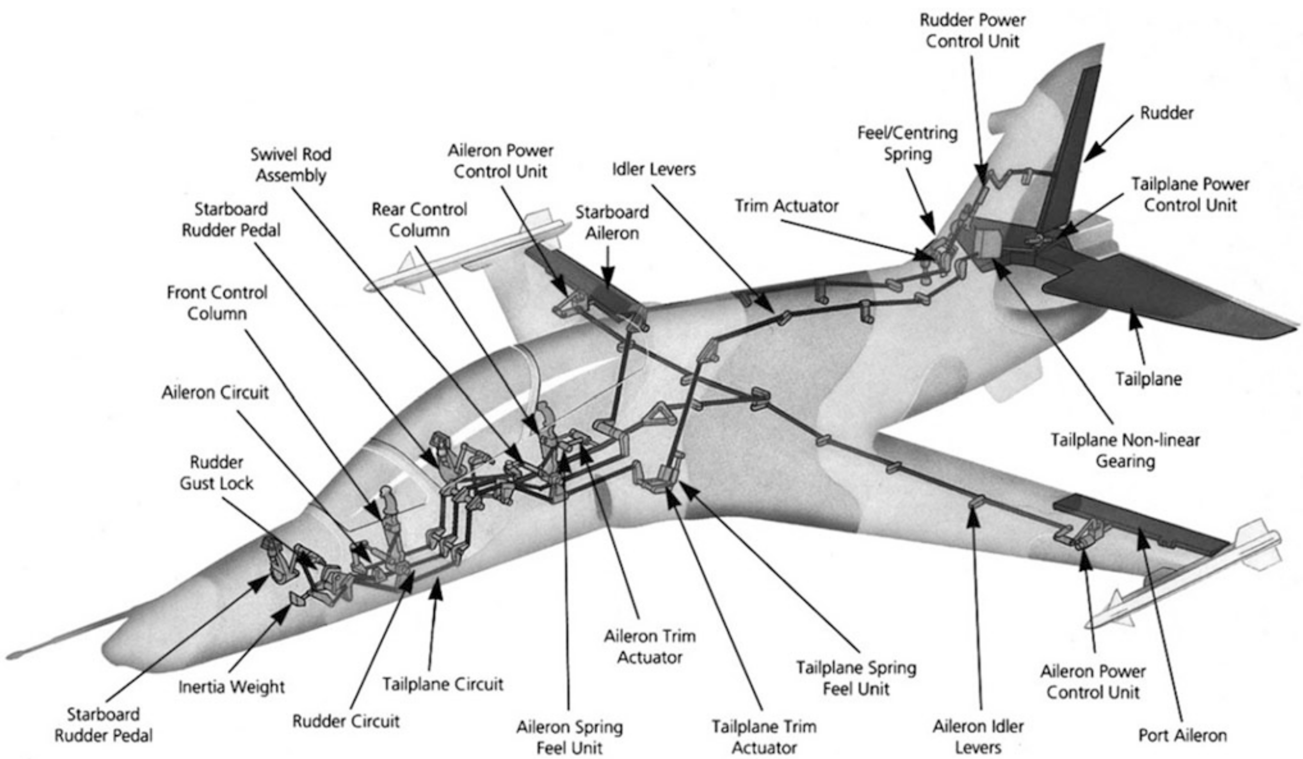

Fig. 3.35 Mechanically signalled flight control system. (Courtesy of BAE Systems)

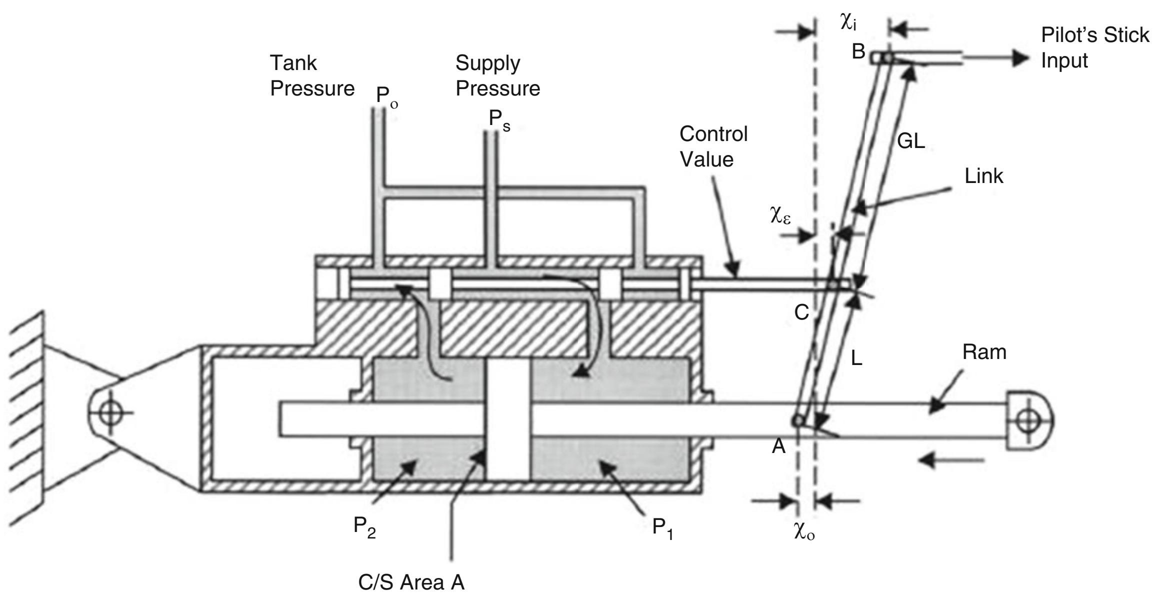

Fig. 3.36 Power Control Unit operation

The PCU uses a tandem arrangement of actuators and servo control valves operated from two totally independent hydraulic supplies to meet the safety and integrity requirements. Mechanically signalled PCUs are extremely reliable systems which have accumulated a vast operating experience, as they are universally installed in modern military and civil jet aircraft.

3.7.2 PCU Transfer Functions

Referring to Fig. 3.36, movement of the pilot's control column, x_i, causes the link AB to pivot about A.

This produces a valve movement which is equal to

$$\frac{l}{Gl+l}\cdot x_i$$

That is

$$\frac{1}{G+1}\cdot x_i$$

Once the spool valve ports have opened, flow passes to the ram, which starts to move in the opposite direction. This causes the link to pivot about B and produces a valve movement equal to

$$\frac{Gl}{Gl+l}\cdot x_0$$

where x_0 is the actuator displacement, that is

$$\frac{G}{G+1}\cdot x_0$$

Hence, the net valve opening, x_ε, is given by

$$x_\varepsilon = \frac{1}{G+l}(x_i - Gx_0) \tag{3.72}$$

(G is the stick-to-actuator gearing).

The relationship between ram velocity, $\dot{x}_0$, and valve opening, x_ε, can be derived as follows, by making the following assumptions:

(i) The spool valve has square ports of equal area so that the uncovered valve port area, a, is directly proportional to the spool valve displacement, x_ε, from the closed position, that is $a = K_1 x_\varepsilon$, where K_1 is a constant which is dependent on the valve dimensions.

(ii) The hydraulic fluid is assumed to be incompressible.

(iii) The external forces acting on the ram are small, that is the ram is unloaded, and control surface inertia can be ignored. (The load inertia torques are generally fairly small in comparison with the actuator torque, which can be exerted.)

(iv) The exhaust (or tank) pressure, P_0, of the hydraulic supply is normally atmospheric pressure, which is small in comparison with the supply pressure, P_s, so that P_0 can be neglected.

It can be shown by Bernoulli's equation that the velocity, V, of the fluid flowing through an orifice is directly proportional to the square root of the pressure difference across the orifice, that is,

$$V = K_2\sqrt{\text{Pressure difference}}$$

where K_2 is a constant which is dependent on the density of the fluid and which also takes into account losses at the orifice (Discharge Coefficient). Flow through the orifice, $Q = aV$. Hence, flow to actuator is $K_1K_2x_\varepsilon\sqrt{P_s - P_1}$. Flow from actuator to exhaust is $K_1K_2x_\varepsilon\sqrt{P_2 - P_0} = K_1K_2x_\varepsilon\sqrt{P_2}$ as P_0 is assumed to be zero.

The flows into and out of the actuator are equal so that $P_2 = (P_s - P_1)$, and, neglecting external loads and the load inertia, $P_1A = P_2A$, where A is the ram cross-sectional area. Hence, $P_1 = P_2 = P_s/2$.

Flow through the valve orifices, Q, is equal to the displacement flow created by the ram movement, that is $Q = A\dot{x}_0$. Whence $A\dot{x}_0 = K_1K_2\sqrt{P_s/2}\cdot x_\varepsilon$, that is,

$$\dot{x}_0 = K_v x_\varepsilon \tag{3.73}$$

where K_v is the actuator velocity constant $K_1K_2\frac{\sqrt{P_s}}{A\sqrt{2}}$.

Substituting x_ε from Eq. (3.72) yields

$$\dot{x}_0 = K_v\frac{1}{G+1}(x_i - Gx_0) \tag{3.74}$$

from which

$$\frac{x_0}{x_i} = \frac{1}{G}\cdot\frac{1}{(1+T_{Act}D)} \tag{3.75}$$

where T_{Act} is the actuator time constant $= (G + 1)/GK_v$.

Hence, the actuator transfer function is a simple first-order lag.

Typical values for a PCU time constant are around 0.1 s. This corresponds to a bandwidth (−3 dB down) of 1.6 Hz approx. (10 rads/s).

The phase lag at 1 Hz is often used as a measure of the actuator performance and would be 32° in the above case.

3.8 Stability Augmentation Systems

3.8.1 Limited Authority Stability Augmentation Systems

The possible need for improved damping and stability about all three axes has been referred to in the preceding sections. This can be achieved by an auto-stabilisation system, or, as it is sometimes referred to, a stability augmentation system.

Yaw stability augmentation systems are required in most jet aircraft to suppress the lightly damped short-period yawing motion and the accompanying oscillatory roll motion due to yaw/roll cross-coupling known as Dutch roll motion, which can occur over parts of the flight envelope (refer to Sect. 3.6.4). In the case of military aircraft, the yaw damper system may be essential to give a steady weapon aiming platform as the pilot is generally unable to control the short-period yawing motion and can in fact get out of phase and make the situation worse.

A yaw damper system is an essential system in most civil jet aircraft as the undamped short-period motion could cause considerable passenger discomfort.

As mentioned earlier, a yaw damper system may be insufficient with some aircraft with large wing sweepback to suppress the effects of the yaw/roll cross-coupling and a roll damper (or roll stability augmentation) system may also be necessary. The possible low damping of the short-period pitch response (refer to Sect. 3.5) can also require the installation of a pitch damper (or pitch stability augmentation) system. Hence, three-axis stability augmentation systems are installed in most high-performance military jet aircraft and very many civil jet aircraft.

A single channel, limited authority stability augmentation system is used in many aircraft, which have an acceptable though degraded and somewhat lightly damped response over parts of the flight envelope without stability augmentation. 'Single channel' means that there is no back-up or parallel system to give a failure survival capability.

The degree of control, or authority, exerted by the stability augmenter is limited so that in the event of a failure in the stability augmentation system, the pilot can over-ride and disengage it. Typical authority of the stability augmentation system is limited to a control surface movement corresponding to $\pm 0.5\ g$.

A simple stability augmentation system is shown schematically in Fig. 3.37. It comprises a rate gyroscope which senses the angular rate of rotation of the aircraft about the auto-stabilised axis and which is coupled to an electronic unit which controls the stability augmentation actuator. The stability augmentation actuator controls the main servo actuator (driving the control surface) in parallel with the pilot's control by means of a differential mechanism – typically a lever linkage differential.

The control surface angular movement is thus the sum of the pilot's stick input and the stability augmentation output. The stability augmentation system produces a control surface movement which is proportional to the aircraft's rate of rotation about the axis being stabilised and hence a damping moment proportional to the angular rate of rotation of the aircraft about that axis. In effect a synthetic $N_r r$ or $L_p p$ or $M_q q$ term. In practice, the stability augmentation damping term is more complicated than a simple (constant) × (aircraft rate of rotation) term because of factors such as stability augmentation servo performance and the need to avoid exciting structural resonances, that is, 'tail wagging the dog' effect. This latter effect is due to the force exerted by the control surface actuator reacting back on the aircraft structure, which has a finite structural stiffness.

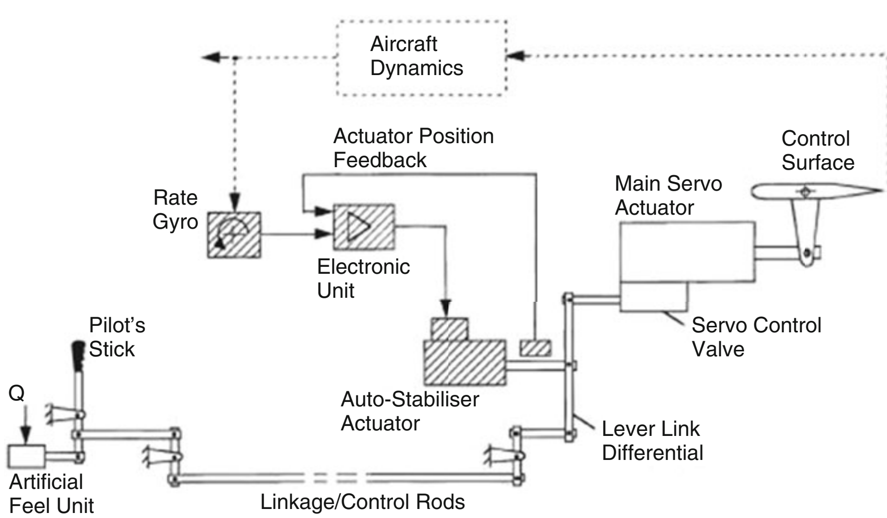

Fig. 3.37 Simple stability augmentation system

The resulting bending of the aircraft structure may be sensed by the stability augmentation rate gyro sensor and fed back to the actuator and so could excite a structural mode of oscillation, if the gain at the structural mode frequencies was sufficiently high. In the case of stability augmentation systems with a relatively low-stability augmentation gearing, it is generally sufficient to attenuate the high-frequency response of the stability augmentation with a high-frequency cut-off filter to avoid exciting the structural modes. The term 'stability augmentation gearing' is defined as the control surface angle/degree per second rate of rotation of the aircraft.

With higher-stability augmentation gearings, it may be necessary to incorporate '*notch filters*', which provide high attenuation at the specific body mode flexural frequencies. (This is briefly covered again in Chap. 4.)

Most simple, limited authority yaw dampers feed the angular rate sensor signal to the stability augmentation actuator through a 'band pass filter' with a high-frequency cut-off (see Fig. 3.38). The band pass filter attenuation increases as the frequency decreases and becomes infinite at zero frequency (i.e. DC) and so prevents the stability augmentation actuator from opposing the pilot's rudder commands during a steady rate of turn. (This characteristic is often referred to as 'DC blocking'.) The yawing motion frequency is in the centre of the band pass range of frequencies. The angular rate sensor output signal resulting from the short-period yawing motion thus passes through the filter without attenuation or phase shift and so provides the required signal to the stability augmentation actuator to damp the oscillatory yawing motion. (It should be noted that this type of filter in flight control systems is often referred to as a 'wash-out filter', particularly in the USA, as it effectively 'washes out' the DC response.)

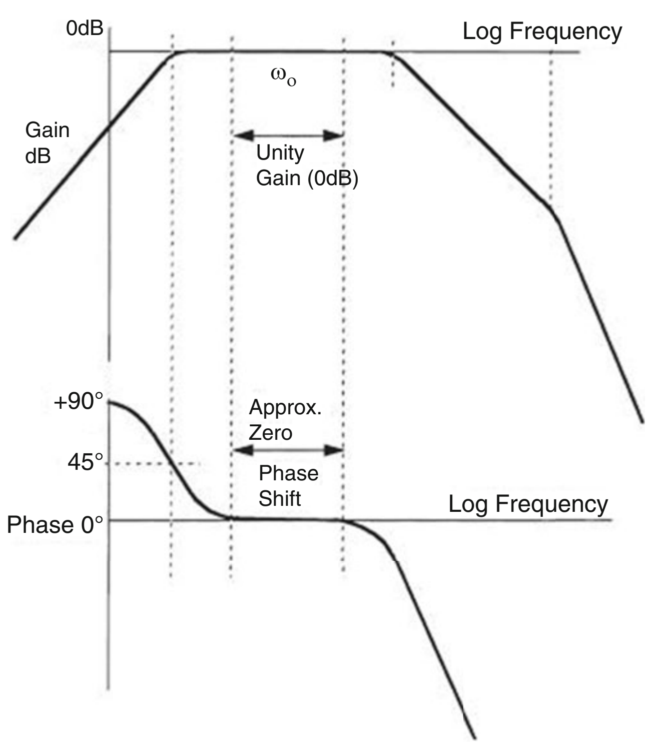

Fig. 3.38 DC blocking or 'wash-out' filter with high-frequency cut-off

The variation in the aircraft response and control effectiveness over the flight envelope may require the stability augmentation gearings to be switched as a function of height and airspeed to possibly two or three different values.

3.8.1.1 'Worked Example' of Simple Pitch Stability Augmentation

An example of a typical representative simple pitch stability augmentation is given below to show how initial calculations can be made to obtain an order of magnitude estimate of the stability augmentation 'gearing' required using the transfer functions derived in Sect. 3.5 (stability augmentation 'gearing' being the tailplane angle in degrees per degree/s rate of pitch). It should be pointed out that much more complex computer modelling and simulation is necessary to establish the optimum values and allow for a more complex transfer function. For example:

(a) Certain derivatives have been ignored.
(b) Lags in the actuator response have been neglected together with any non-linear behaviour which might be present.
(c) The transfer functions of any filters required to attenuate rate gyro noise and avoid excitation of structural resonances have been omitted.

Referring to Sect. 3.5.4, pitch rate, q, to tailplane angle, η, transfer function is

$$\frac{q}{\eta} = \frac{K(1 + T_2 D)}{\left(D^2 + 2\zeta\omega_0 D + {\omega_0}^2\right)}$$

where $T_2 = mU/Z_\alpha$ and $K = M_\eta/I_y T_2$.

Referring to Fig. 3.39 (ignoring lags in auto-stab actuator, main actuator, gyro and filters, etc.):

Stability augmentation output is G_qq

$$\text{Tailplane angle}, \eta = \delta_i - G_q q \qquad (3.76)$$

where G_q is stability augmentation gearing and δ_i is the pilot's stick input. Whence

$$q = \frac{K(1 + T_2 D)}{\left(D^2 + 2\zeta\omega_0 D + \omega_0^2\right)} \cdot \left(\delta_i - G_q q\right)$$

from which

Fig. 3.39 Pitch stability augmentation loop

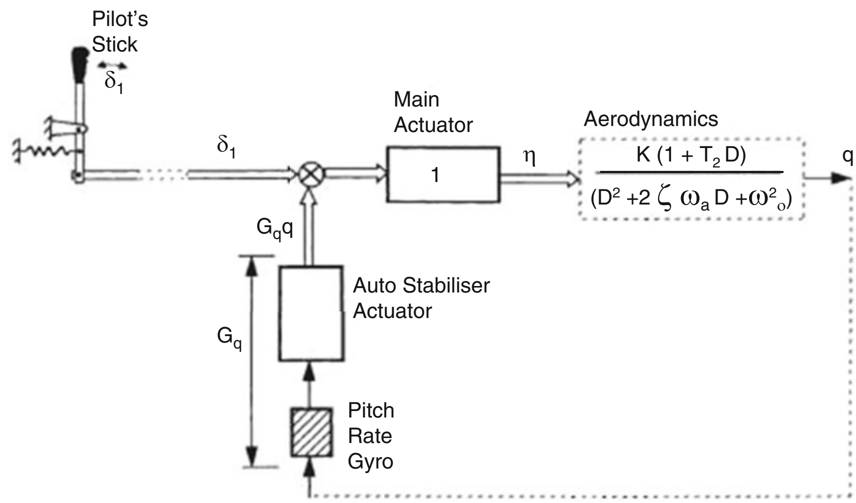

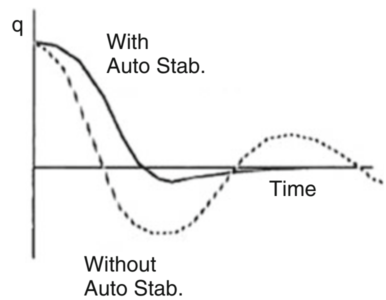

Fig. 3.40 Pitch response with and without stability augmentation

$$\left[D^2 + \left(2\zeta\omega_0 + KT_2G_q\right)D + \left({\omega_0}^2 + KG_q\right)\right]q = K(1 + T_2D)\delta_i$$

The worked example in Sect. 3.5.2 provides the data for the basic aircraft response with $K = 87$, $T_2 = 0.67$, $\omega_0 = 6$ rad/s, $\zeta = 0.2$.

The required value of G_q to improve the damping of the aircraft's pitch response to correspond to a damping ratio of 0.7 is derived below.

Let $\omega_{0\ \text{stab}}$ and ζ_{stab} denote the undamped natural frequency and damping ratio of the quadratic factor in the transfer function q/δ_i of the aircraft with pitch stability augmentation.

Hence

$$\omega_{0\ \text{stab}}^2 = \omega_0^2 + KG_q$$
$$2\zeta_{\text{stab}}\omega_{0\ \text{stab}} = 2\zeta\omega_0 + KT_2G_q$$
$$\zeta_{\text{stab}} = 0.7$$

$\therefore 2 \times 0.7 \times \omega_{0\ \text{stab}} = (2 \times 0.2 \times 6) + (87 \times 0.67 \times G_q)$, whence $\omega_{0\ \text{stab}} = 1.71 + 41.6G_q$, viz. $1734G_q^2 + 55G_q - 33 = 0$, from which $G_q = 0.12°$ tailplane/degree per second rate of pitch. Whence $\zeta_{\text{stab}} = 0.7$ and $\omega_{0\ \text{stab}} = 6.8$ rad/s (1.1 Hz) approx. The q/δ_i transfer function with stability augmentation is thus

$$\frac{q}{\delta_i} = \frac{87(1 + 0.67D)}{D^2 + 9.5D + 46}$$

The improvement in damping is shown in Fig. 3.39.

It should be noted that the loop gain is only 0.29 – much lower than would be used in an FBW pitch rate command loop (Fig. 3.40).

3.8.2 Full Authority Stability Augmentation Systems

In many cases, aerodynamic performance and manoeuvrability do not always match with stability and damping over the whole of the flight envelope and can lead to restricting compromises. There may thus be a need for full authority stability augmentation over part of the flight envelope (as opposed to the limited authority systems just described). Because the system has full authority, a failure could be catastrophic and so a failure survival system of triplex level redundancy (or higher) is essential.

Triplex level redundancy means three totally independent parallel systems of sensors, electronic units (or controllers) and actuation units with independent electrical and hydraulic supplies.

Basically the triplex system operates on a majority voting of the 'odd man out' principle. Because the three parallel systems or 'channels' are totally independent, the probability of two systems failing together at the same instant in time is negligibly low (of the order typically of 10^{-6}/hour failure probability). A failure in a channel is thus detected by cross-comparison with the two 'good' channels and the failed

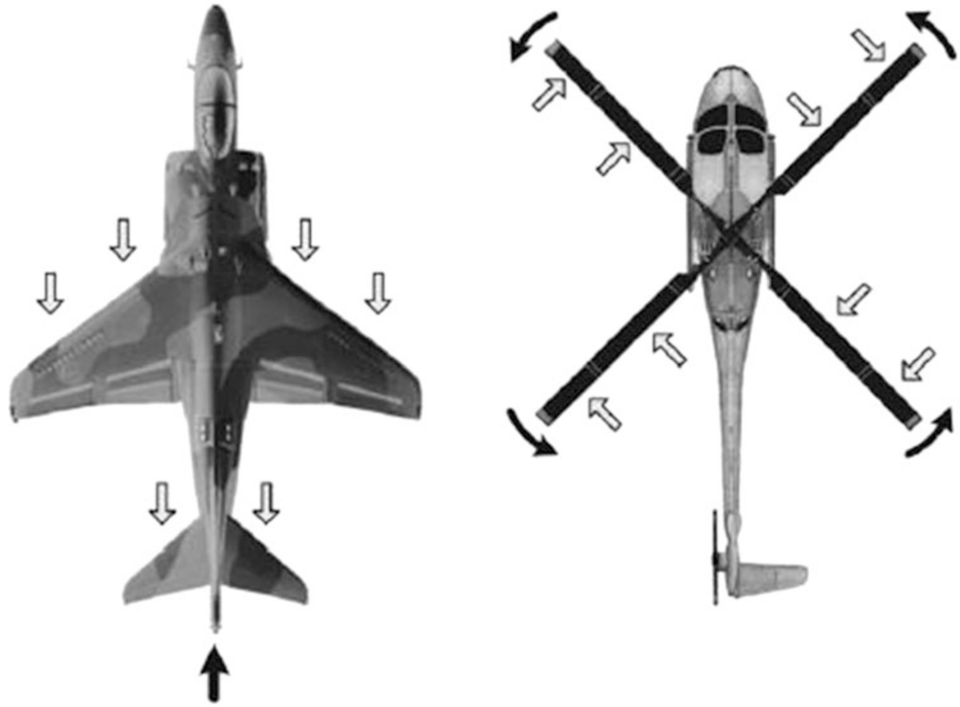

Fig. 3.41 Lift generation: fixed-wing aircraft compared with a helicopter

channel can be disconnected leaving the system at duplex level redundancy. Failure survival redundant configurations are discussed in some detail in Chap. 4, and at this stage it is sufficient to appreciate the basic triplex concept.

A second failure results in a stalemate situation with the failed stability augmentation actuator being counteracted by the 'good' channel. The result is a passive failure situation and the control surface does not move.

The operational philosophy with such a system after the first failure would generally be to minimise the time at risk at duplex level by, say, decelerating and possibly descending until a speed and height condition is reached where stability augmentation is not essential.

The relatively high stability augmentation gearings that may be required together with the failure survival system requirements lead to what is known as a 'manoeuvre command fly-by-wire' flight control system. This is discussed in Chap. 4.

3.9 Helicopter Flight Control

3.9.1 Introduction

The aim of this section is to explain the basic principles of helicopter flight control including stability augmentation. This provides the lead-in to helicopter fly-by-wire control systems, which are covered in Chap. 4.

Like fixed-wing aircraft, helicopters depend on the aerodynamic lift forces resulting from the flow of air over the wing surfaces, in this case, the rotor blades. The airflow over the wings of a fixed-wing aircraft is a result of the forward speed of the aircraft as it is propelled by the thrust exerted by the jet engines, or propellers.

In the case of the helicopter, however, the airflow over the wings (rotor blades) is caused by the rotation of the whole rotor system; thus, the aircraft need not move.

Figure 3.41 illustrates the fundamental difference between fixed-wing aircraft and rotary wing aircraft (helicopters) in the generation of aerodynamic lift.

This gives the helicopter the major advantages of being able to take-off and land vertically, move forward or backwards, move sideways, and the ability to hover over a fixed point.

These capabilities are widely exploited in both civil and military helicopter usages. For example, civil applications such as air ambulances, police surveillance, air–sea rescue, and transporting passengers to and from locations with restricted space.

Military applications include operations by special forces in inaccessible terrain, transport of troops and equipment where roads are poor, possibly mined and subject to ambush, evacuation of the wounded, and ground attack (helicopter gunships). Naval applications include anti-submarine operations, airborne early warning, shipping strikes using air-launched guided missiles, and ship-to-ship or ship-to-shore transport of men and equipment.

There are a number of basic rotor configurations which are used in helicopters. These are described briefly below.

Fig. 3.42 Single main rotor configuration – AgustaWestland AW 159 'Lynx Wildcat' helicopter. (Courtesy of AgustaWestland)

Single Main Rotor This is the most common and widely used rotor configuration. An essential feature of this configuration is a means of applying a torque about the yaw axis to counteract the reaction torque acting on the fuselage to the turning of the main rotor. This is usually achieved with a tail rotor driven from the engine(s), the yawing moment being controlled by changing the pitch of the tail rotor blades. An alternative method is the 'NOTAR'[1] system, which uses the reaction torque from a jet of air supplied from the engine compressor.

The rotor can comprise two blades, three blades, four blades or even five blades depending on the size and roles of the particular helicopter.

Figure 3.42 shows an example of a single main rotor helicopter configuration and is an illustration of the new AgustaWestland AW 159 'Lynx Wildcat' army/naval helicopter, which made its first flight in November 2009 at Yeovil, Somerset. This new helicopter is a development of the well-proven Westland WG 13 'Lynx' helicopter, which first entered service with the Royal Navy and the British Army over 30 years ago and has since been exported worldwide.

Co-axial Rotor Configuration with Contra-Rotating Rotors This configuration eliminates the rotor reaction torque problem and dispenses with the need for a tail rotor. The new Sikorsky S 97 'Raider' light assault helicopter, currently under construction, exploits the co-axial contra-rotating rotor configuration together with a pusher propeller providing forward thrust. The basic configuration is shown in Fig. 3.43. This configuration is used in the earlier Sikorsky 'X-2 Technology Demonstrator', which has demonstrated a level speed of over 250 knots.

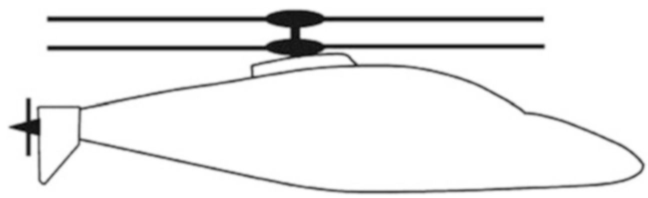

Fig. 3.43 Co-axial contra-rotating rotors configuration – Sikorsky S 97 helicopter

Yaw control is achieved by increasing the collective pitch of one rotor and reducing it on the other rotor to produce a torque about the yaw axis.

Contra-rotating rotors reduce the effects of dissymmetry of lift resulting from the forward motion of the helicopter, which increases the lift force on the advancing rotor blades and at the same time decreases the lift on the retreating rotor blades. The increase, or decrease, in lift is at a maximum when the rotor blade is at 90 to the direction of forward motion. The effects are reduced because the two rotors are turning in opposite directions causing the blades to advance on either side at the same time.

Other benefits include increased payload for the same engine power as all the engine power is available for lift and thrust, whereas some of the engine power is required to drive the anti-torque rotor on a single rotor design. The configuration can also be more compact overall. The principal disadvantage is the increased mechanical complexity.

Contra-Rotating Tandem Rotor Configuration Another configuration which eliminates the rotor reaction torque problem is the contra-rotating tandem rotor configuration. The well-proven Boeing Chinook helicopter illustrated in Fig. 3.44 is a good example of this configuration.

Yaw control is achieved by differential main rotor torque.

[1]NOTAR is an acronym for 'No Tail Rotor'.

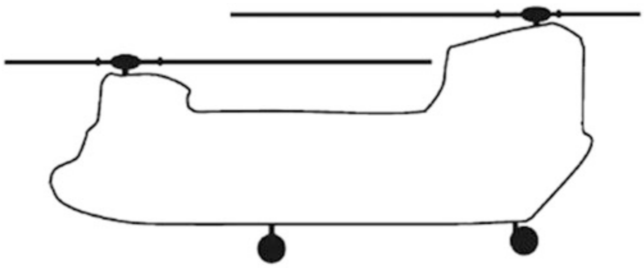

Fig. 3.44 Tandem rotor configuration – Boeing Chinook helicopter

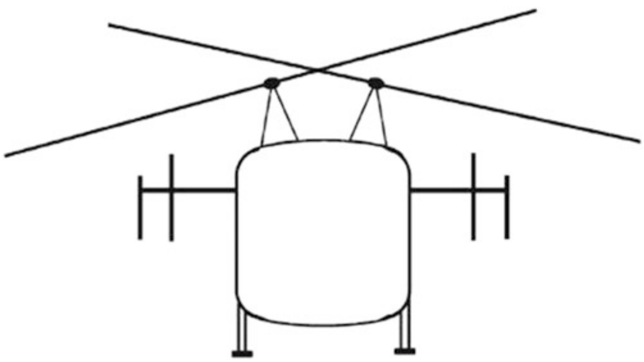

Fig. 3.45 Intermeshing rotor configuration – Kaman helicopter

Intermeshing Contra-Rotating Rotor Configuration This configuration also has zero net rotor reaction torque. Figure 3.45 shows the intermeshing rotor system developed by the Kaman helicopter company in the USA. The new Kaman K-Max helicopter exploits this configuration and features an impressive lifting capability. Yaw control is achieved by differential rotor torque.

The methods adopted for attaching the rotor blades to the rotor head have a direct influence on the dynamic response of the helicopter and can be divided into three basic categories, comprising:

- Articulated rotors
- Semi-rigid rotors
- Rigid rotors

Articulated Rotor Head Fig. 3.46 illustrates the drag-and-flapping hinge design of the rotor head.

The flapping hinges give the rotor blades limited freedom about the flapping hinges to move up or down as the lift increases on the advancing rotor blade and decreases on the retreating rotor blade.

It should be appreciated that there are large centrifugal forces exerted on the rotor blades due to their rotational velocity. These centrifugal forces oppose the deflection of the rotor blades from the plane of rotation normal to the rotor drive shaft.

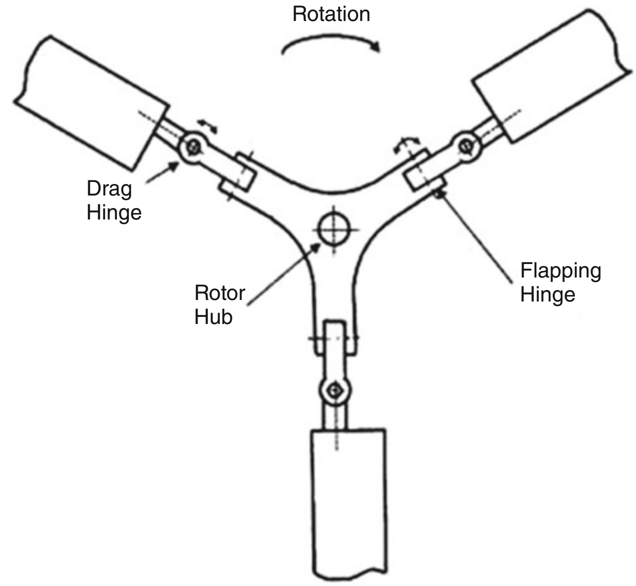

Fig. 3.46 Drag-and-flapping hinges on an articulated rotor

The rotor blades thus deflect from this normal plane until the moment about the flapping hinge due to the rotor lift force is balanced by the moment due to the centrifugal force component normal to the rotor blade.

The drag hinges, also known as 'lead-lag' hinges, allow the rotor blades to move freely backward and forward by a limited amount in the plane of rotation relative to the other blades (or the rotor head). The flapping-and-drag hinges enable a lighter mechanical rotor head to be used; the down side is the increased mechanical complexity and wear and maintenance of the hinge bearings.

Semi-Rigid Rotors The semi-rigid rotor is illustrated schematically in Fig. 3.47, and is an integral rotor unit, without blade articulation.

There are no flapping or drag hinges but it has, however, limited flexibility in the flapping-and-drag planes. As in all helicopters, the flexibility of the long, relatively thin rotor blades enables them to bend up or down under the changing lift forces.

This configuration eliminates the mechanical complexity of flapping-and-drag hinges and reduces the bending moments on the rotor shaft. It also has a much faster pitch attitude response and enables high manoeuvrability to be achieved (in conjunction with the command/stability augmentation system). There are many examples of helicopters in service with semi-rigid rotors, for example the 'Lynx' helicopter.

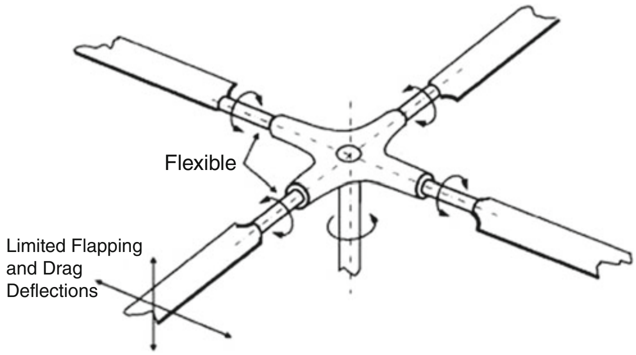

Fig. 3.47 Semi-rigid rotor

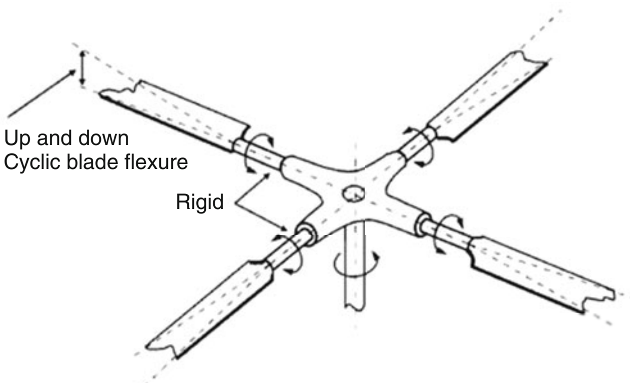

Fig. 3.48 Rigid rotor

Rigid Rotors This is also an integral rotor unit with very much less blade flexibility. Figure 3.48 illustrates a rigid rotor configuration.

3.9.2 Control of the Helicopter in Flight

Control of the flight path of a helicopter is achieved by controlling the angle of incidence of the individual rotor blades to the airstream, that is, their *pitch angle*. This is achieved by means of a swash plate mechanism.

The basic swash plate mechanism is illustrated schematically in Fig. 3.49.

The lower half of the swash plate mechanism comprises a co-axial collar which can move axially up or down with respect to the rotor head. The co-axial collar, in turn, incorporates a spherical bearing which enables the lower swash plate to tilt about the centre of rotation of this bearing. The lower swash plate can thus move axially up or down and can also be independently tilted at an angle to the helicopter fore and aft axis, or the helicopter lateral axis. Actuators control the up or down axial movement and the fore and aft, and lateral, tilt of the lower swash plate. The upper swash plate, which is coupled to the rotor shaft by a scissor linkage, in turn controls the individual rotor blade pitch angles through the pitch linkage arms.

Fig. 3.49 Schematic diagram of the swash plate mechanism

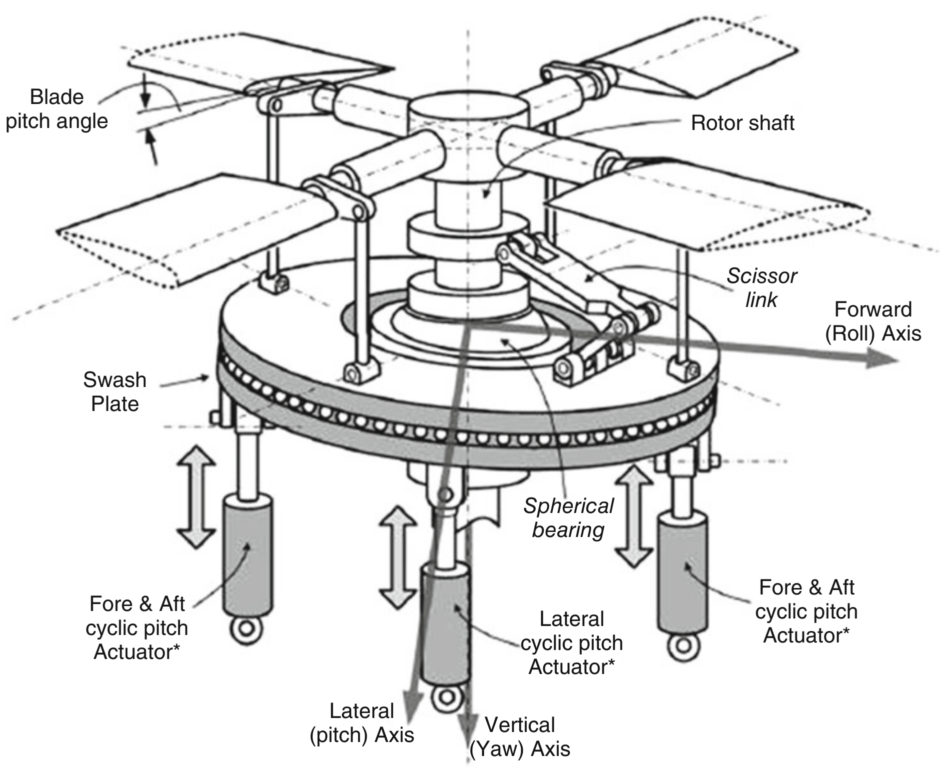

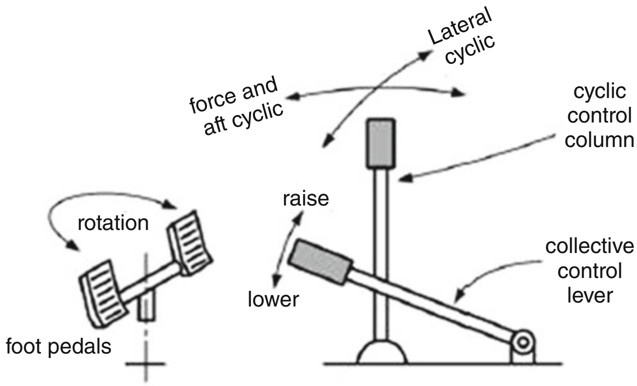

Fig. 3.50 Pilot's controls

Pilot's Controls Fig. 3.50 illustrates the layout of the pilot's controls.

The pilot has a *collective* control lever, usually located on the left side, to control the vertical motion of the helicopter by changing the rotor collective pitch angle.

There is a *cyclic* control column to control the fore and aft and lateral motion of the helicopter by changing the cyclic pitch angles of the rotor blades.

Collective and cyclic pitch control will be explained in the next sections.

There is also a *foot pedal* control for the pilot to control the pitch angle of the variable pitch tail rotor and hence the yawing moment (and side force) it exerts.

It should be noted that the rotor speed is controlled automatically, in modern helicopters, and is maintained at a sensibly constant value in a particular flight mode. This is governed by the limits set by the advancing rotor blade tip velocity not becoming supersonic and the retreating rotor blades not stalling.

The rotor lift is thus mainly determined by the rotor collective pitch angle.

Collective Pitch Control Operating the pitch control lever raises or lowers the collar of the lower part of the swash plate thereby changing the pitch angle of each rotor blade by the same amount, simultaneously. Refer to Fig. 3.49.

Increasing the collective pitch angle increases the rotor lift and the helicopter climbs; similarly, decreasing the rotor pitch angle reduces the rotor lift so the helicopter descends. The helicopter can be maintained in a hovering condition by adjusting the rotor lift to exactly balance the helicopter's weight.

It is, however, also necessary to adjust the tail rotor pitch angle to counter the change in the rotor reaction torque acting on the helicopter about the yaw axis, when the rotor collective pitch angle is changed.

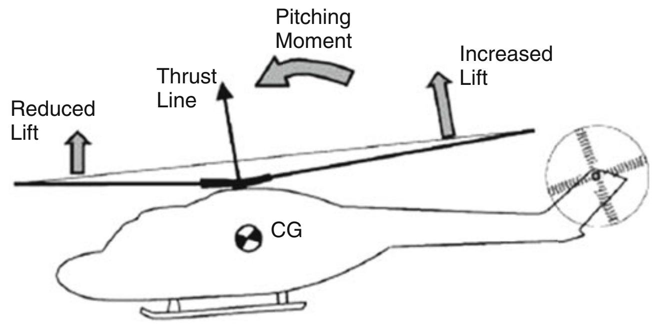

Fig. 3.51 Forces and moments acting on the helicopter

Cyclic Pitch Control Forward flight (and also rearward or sideways flight) is achieved by cyclic pitch control and is explained in the next subsections.

Pitch Axis Control Forward movement of the pilot's control column causes the front of the lower swash plate to tilt downwards with respect to the fore and aft axis.

The rotor blade pitch angles thus change cyclically over each revolution of the rotor, as shown in Fig. 3.49. The pitch angle of each advancing rotor blade is progressively decreased as it approaches the fore and aft position, so that the lift force is reduced at the front of the rotor disc. At the same time, the pitch angle of each retreating rotor blade is increased as it approaches the rear of the fore and aft axis thereby increasing the lift force on the rear half of the rotor disc.

The rotor disc is thus deflected about the helicopter pitch axis. In simple terms the deflected rotor disc results in both a horizontal fore and aft force and a pitching moment. The resulting attitude response is very much influenced by the rotor design, which can vary between very rigid and very flexible, as explained earlier.

The more rigid the rotor attachment, the more moment is imparted to the aircraft, so this results in a rapid change in pitch attitude.

Figure 3.51 illustrates the forces and moments acting on the helicopter.

The longitudinal force is dominant in the case of the more flexible rotor attachment, and this is applied to the rotor mast head. The attitude change develops as the helicopter accelerates forward to a constant speed when the forces and moments at the mast head cancel out, as shown in Fig. 3.52.

In general, at a given forward velocity there will be a corresponding pitch angle, that is, the greater the speed, the more the nose-down attitude. In equilibrium, the forward component of rotor force is balanced by the aerodynamic drag force.

It should be noted that the pitch control of a helicopter is more complex than that of a fixed-wing aircraft, where the short-period dynamics can be represented as a simple second-order system, as explained earlier in this chapter.

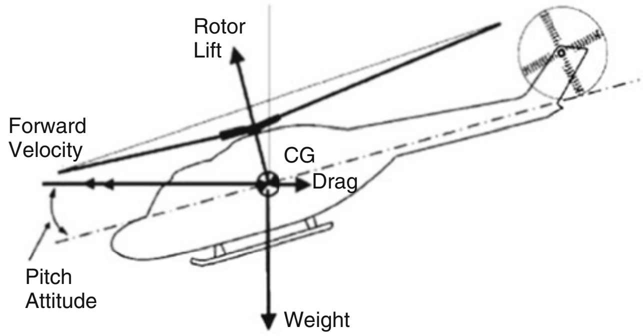

Fig. 3.52 Steady-state forward motion

In contrast, the pitch axis control depends on the rotor dynamics, the helicopter rigid body dynamics and the resultant effect of the airspeed. The pitch axis motion of a helicopter has been described as the equivalent to a fixed-wing aircraft with an unstable short-period phugoid.

Roll axis This is similar to the pitch axis (at least at low speed around the hover) in that roll stick deflection results in a lateral tilt of the rotor disc, followed by a bank angle and a lateral acceleration. At higher speed, the bank angle results in a side force and hence (ideally) a coordinated turn, although this involves appropriate control of the tail rotor and the collective axes of operation.

Yaw Axis The pilot's pedals provide a yawing moment (also a side force) via the variable pitch tail rotor, so that the helicopter rotates about a vertical axis. As the airspeed increases, the natural weathercock stability of the airframe comes into effect, and the function of the pedals and the tail rotor is to minimise sideslip, hence helping turn coordination during banked turns.

3.9.3 Stability Augmentation

Controlling the flight path of a basic helicopter (without stability augmentation) can present the pilot with a relatively high workload in certain flight conditions. It can involve the simultaneous coordination of the following:

Fore and aft and lateral motion of the helicopter through the control column cyclic pitch control system

Lift control through the collective pitch control lever

Control of yawing motion through the foot pedals

The pitch attitude response can have neutral stability, or even be divergently unstable without the intervention of the pilot in the loop. A basic Stability Augmentation System (SAS) may thus be required to give the helicopter good control and handling characteristics. The helicopter is also basically asymmetric and this requires cross-axis coupling in various areas to suppress these effects; for instance, collective to yaw and collective to pitch.

Less sophisticated helicopters have a single channel, or simplex, limited authority three-axis stability augmentation system providing pitch, roll, yaw rate damping about the respective pitch, roll, yaw axes. The system is basically similar to the fixed-wing stability augmentation system shown in Fig. 3.37; the stability augmentation actuators in this case coupling into the fore and aft, and lateral, cyclic pitch and tail rotor pitch main actuators (or Power Control Units [PCUs] as they are generally called). Washed-out, or DC-blocked, pitch attitude and roll attitude signals are frequently included in the pitch and roll channels.

The actuator authority, in the case of a simplex system, is set at a value which limits the magnitude of the disengagement transient to a safe acceptable level, following a failure in the stability augmentation system.

This inevitably limits their capability, and more sophisticated systems which require larger actuator authority employ fault tolerant system architectures.

Figure 3.53 (**a**, **b**, **c**) illustrates the various fault tolerant SAS architectures comprising duplex, dual–dual and triplex systems.

A duplex system is shown in Fig. 3.53a. All axes have two entirely independent lanes operating in such a manner that the resultant blade angle change produced in response to sensor outputs is the average of the two individual lanes. Under normal operating conditions the two lanes are so matched as to be practically identical. The outputs of the Computer and the lane actuator position in each lane are continually monitored and cross-compared. Any significant disparities are displayed to the pilot on the Controller and Monitor Unit and the pilot can disengage the stability augmentation system.

The duplex architecture ensures that a lane failure results in only a 'passive' failure of the system; that is, the summed output of the two lane actuators remains at the position it was in at the time of the failure. This minimises the disengagement transient when a failure occurs and the system reverts to manual control.

The dual–dual system (Fig. 3.53b) is basically a dual version of the duplex system. It can survive the first failure and reverts to manual control with minimal transient in the event of a second failure. This is a low-probability event, and very rarely will the pilot be without the handling and control benefits of the system.

The triplex system shown in Fig. 3.53c is able to survive the first failure, and reverts to a duplex system. The second failure is a passive failure, with the system reverting to manual operation with minimal transient.

Modern stability augmentation systems are implemented digitally and have a very much higher reliability than the older analogue systems. They also incorporate efficient and effective self-monitoring and self-test facilities.

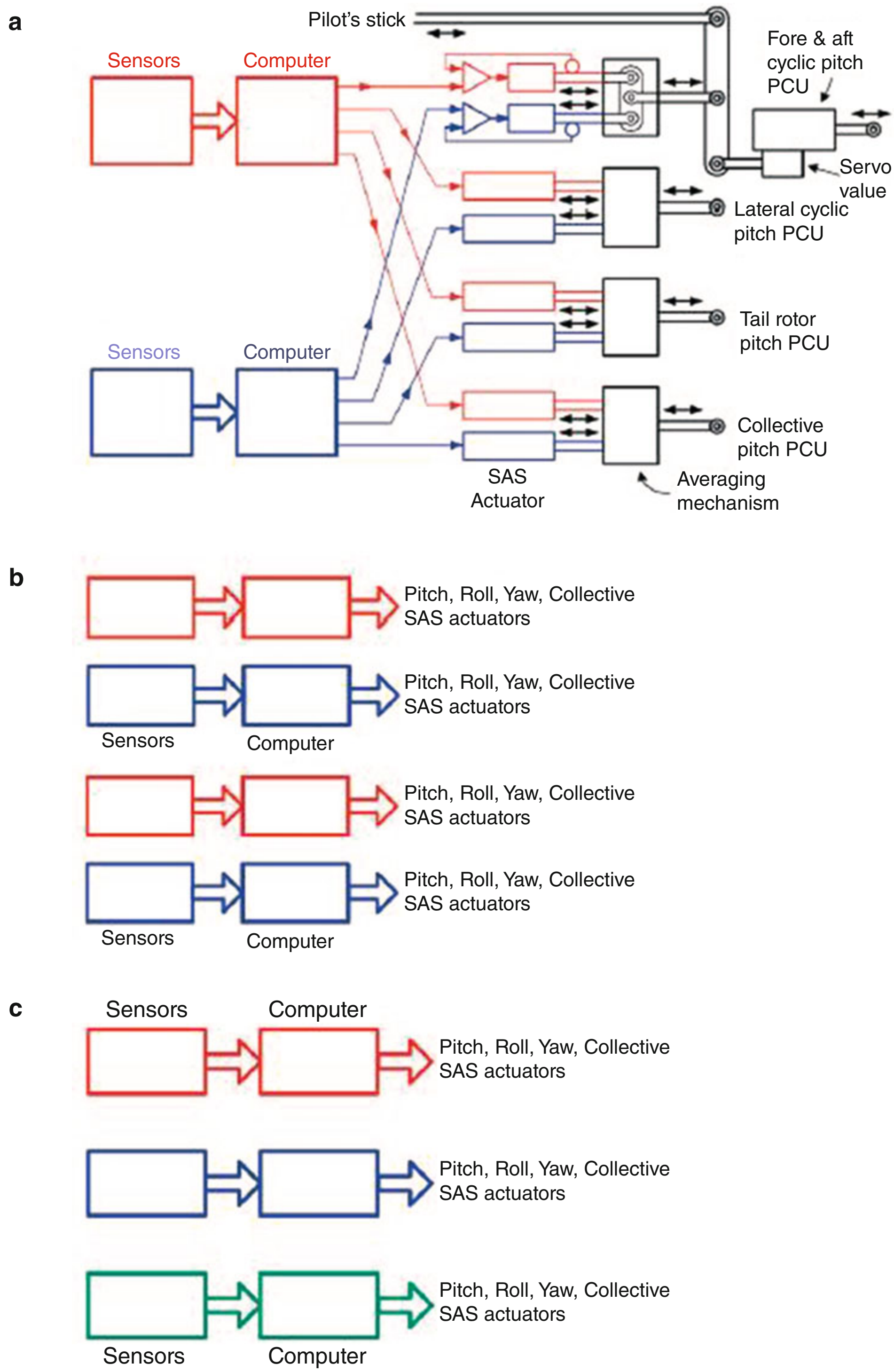

Fig. 3.53 (**a**) Duplex stability augmentation system; (**b**) Dual–dual stability augmentation system; (**c**) Triplex stability augmentation system

Angular momentum gyro-based sensor systems have been replaced with strap-down Attitude/Heading Reference Systems (AHRS) using solid state rate gyros and accelerometers. They provide pitch, roll attitude and heading data together with pitch, roll, yaw rates and forward, lateral, normal acceleration components from the one unit (refer Chap. 5). The MTBF of a strap-down AHRS is in the region of 50,000 hours, compared with an angular momentum gyro-based sensor system with an MTBF of around 2500 hours.

3.9.3.1 Fault Tolerant Pitch Axis Stability Augmentation

The helicopter load can result in the centre of gravity (CG) being offset from the rotor thrust line. This requires an increase in the cyclic pitch angle to provide a balancing trim moment and hence increased stick force. (Stick force is proportional to stick deflection and hence cyclic pitch angle.) The CG offset can also change in flight; for example, hovering over a fixed spot and lowering a crew member and

Fig. 3.54 Pitch axis stability augmentation system

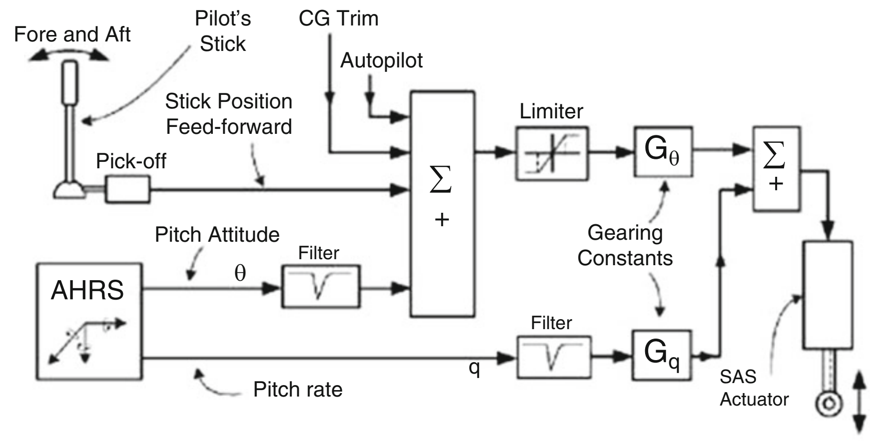

winching up a casualty in a rescue operation. The stick deflection to pitch attitude relationship thus changes when the CG offset changes.

Fault tolerant, pitch axis stability augmentation systems augment the characteristic stick deflection to attitude change. Figure 3.54 illustrates a single channel of a typical fault tolerant pitch system. Command augmentation is provided by stick position feed forward (or 'stick cancellation'), whilst stability augmentation and damping is provided by pitch attitude and pitch rate feedback. The command augmentation system is normally set up to match the normal stick to attitude relationship to minimise disengagement transients.

The augmentation system provides damping and reduces the effects of turbulence. The stability augmentation system opposes and reduces changes in the pitch attitude from that set by the stick position when the helicopter is subjected to a disturbance. The pilot workload to counter a change in CG offset is thus reduced.

A typical system will maintain a constant datum pitch attitude over an approximate ±18° range. Over this range the attitude of the helicopter is proportionally related to the fore and aft cyclic stick position. The stabiliser actuator stroke is limited, so the gearing of blade angle to attitude or stick position has two slopes, with higher gearing over an attitude range of around ±5°.

The AHRS pitch attitude and pitch rate outputs are filtered by structural 'notch' filters to attenuate the harmonic vibration frequencies generated by the rotor rotation, which are sensed by the gyros. ('Notch' filters are covered in Chap. 4.)

An input from the trim wheel enables the pilot to set the null (mid-stroke) position of the stability augmentation actuator.

3.9.3.2 Roll Axis Stability Augmentation

A typical roll axis stability augmentation system is shown in Fig. 3.55, which is similar in many aspects to the pitch axis system. 'Wings'-level attitude is maintained using roll attitude and roll rate information from the AHRS.

Roll attitude is typically proportional to control stick movement for up to about 7° of bank angle and is limited when it reaches that value. Control then reverts substantially to a roll rate system. Large bank angles are achieved and maintained for executing higher *g* turns, by a combination of roll rate and 'washed-out' roll angle. This enables a demanded roll attitude to be maintained.

Because the signal is steady-state DC blocked, it does not permanently saturate the system by demanding a steady-state full actuator stroke. (The stabiliser actuator authority in roll is typically less than ±2° of blade angle.)

The roll angle and roll rate signals need to be filtered by notch filters to attenuate the vibration harmonic frequencies. A further structural 'notch' filter is used to suppress excitation of the rotor lag plane resonance.

A modest amount of phase advance may also be required to achieve acceptable damping. This is because of the cumulative effect of the lags introduced by the notch filters and the PCU actuator response (typically around 1 Hz bandwidth).

The control stick cancellation signals from the stick position pick-offs are typically fed through a simple lag filter. This improves the 'matching' of stick input to attitude and rate attained giving a better response to pilot input.

3.9.3.3 Yaw Axis Stability Augmentation

Figure 3.56 shows a single lane of a basic yaw axis stability augmentation system.

The control signals are passed through notch filters to avoid exciting structural resonance modes. Lateral acceleration signals can be added to improve yaw stability.

3.9.3.4 Collective

Normal acceleration signals from the strap-down AHRS can be used to augment the helicopter pitch stability at high forward speeds and assist autopilot performance.

The normal acceleration signals are typically filtered by a simple lag filter to attenuate higher-frequency noise.

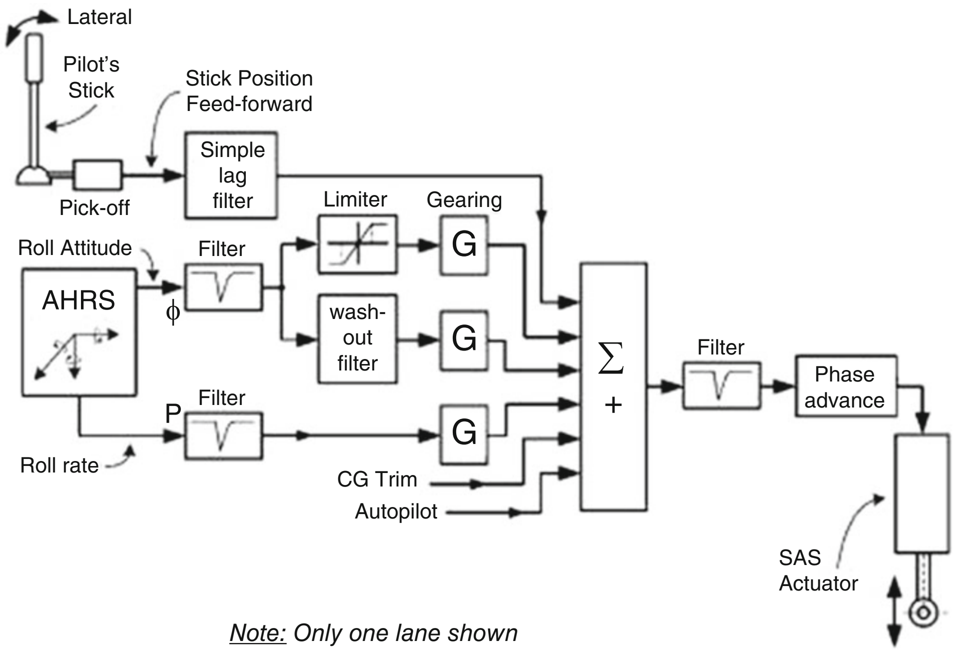

Fig. 3.55 Roll axis auto-stabilisation system

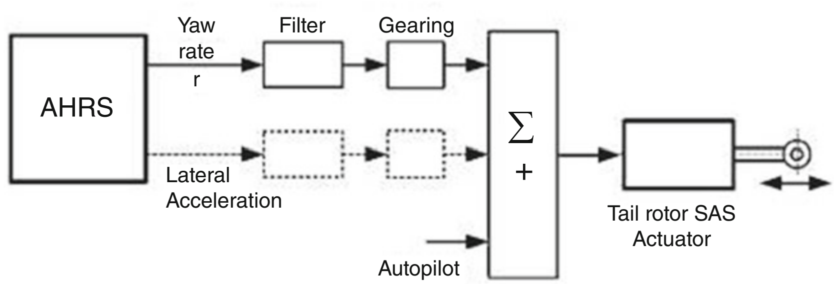

Fig. 3.56 Basic yaw rate stability augmentation system

Fault tolerant stability augmentation systems give a very significant improvement in the control and handling characteristics of the basic helicopter. The improvement, however, is constrained by their limited authority and the need to be able to revert safely to manual control in the event of the loss of the augmentation system.

The full benefits of automatic control require a full authority system which is able to survive two failures in the system from any cause. Replace all mechanical links with electrical links and the system becomes an FBW system similar to those used in fixed-wing aircraft. The all-round improvement in helicopter control and handling characteristics it can confer are covered in the next chapter.

Further Reading

Babister, A.W.: Aircraft Dynamic Stability and Response. Pergammon Press

Bertin, J.J. and Smith, M.L.: Aerodynamics for Engineers, Prentice Hall

Blakelock, J.H.: Automatic Control of Aircraft and Missiles, Wiley

Cook, M.V.: Flight Dynamics Principles. Arnold, Hodder Headline Group (1997)

Dommasch, D.D., Sherby, S.S., Connolly, T.F.: Airplane Aerodynamics. Pitman

Etkin, B.: Dynamics of Atmospheric Flight. Wiley

McLean, D.: Automatic Flight Control Systems. Prentice Hall

McRuer, D., Ashkenas, I., Graham, D.: Aircraft Dynamics and Automatic Control. Princeton University Press

Nelson, R.C.: Flight Stability and Automatic Control. McGraw-Hill

Pratt, R.W.: Flight Control Systems Practical Issues in Design and Implementation, IEE Control Engineering Series, vol. 57. The Institution of Electrical Engineers